"ALEXANDRU IOAN CUZA" UNIVERSITY OF IAŞI

FACULTY OF CHEMISTRY

DOCTORAL SCHOOL OF CHEMISTRY

AZAHETEROCYCLES WITH CONDENSED NUCLEI. SYNTHESIS, STUCTURE, PROPERTIES

PHD THESIS SUMMARY

PhD supervisor,

Univ. Prof. Dr. **Ionel I. MANGALAGIU**

PhD student,

Chemist **Liliana BRĂDĂȚAN**

(married ONICIUC)

2024

Thank you

With great respect and consideration, I would like to express my sincere thanks to those who have offered me scientific support, empathy and a lot of patience during the completion of this doctoral thesis.

In particular, I would like to express my special thanks to the scientific leader ***Prof. univ. dr. Ionel I. Mangalagiu****, for the trust he has given me during all these years, the permanent guidance, the patience he has shown, the effectiv support he has offered during the elaboration of this thesis.*

Thanks to the members of the steering committee, to ***Conf. univ. dr. Vasilichia Antoci****, I thank her from the bottom of my heart for her warmth, patience, and understanding, to* ***Prof. univ. dr. habil. Romeo-Iulian Olariu*** *and* ***Prof. univ. dr. Costel Moldoveanu****, for their precious time, advice and suggestions.*

I would like to thank ***Conf. univ. dr. Dorina Amăriucăi Mantu*** *and* ***C.S. dr. Dumitrela Diaconu****, for their advice and friendship.*

Thanks to ***Prof. univ. dr. Simona-Isabela Dunca*** *for the evaluation of the antimicrobial activity of the compounds synthesized in the Microbiology Laboratory of "Alexandru Ioan Cuza" University of Iasi*

Thanks to the US National Cancer Institute (NCI) for screening anticancer activity on the compounds studied.

Thanks also to the members of the Integrated Centre for Environmental Science Studies for the North-East Development Region (CERNESIM), to ***C.S.III dr. Cătălina Ciobanu*** *for recording the magnetic resonance spectra (MRI) and to A****.C.S dr. Tiberiu Roman*** *for determining the X-ray structures of the compounds.*

Thanks to ***C.S. dr. Laurențiu Valentin Șoroagă*** *for recording the FT-IR spectra and X-ray experiments.*

Thank you to my family, my husband ***Silviu,*** *and my son* ***Alexandru-Ioan*** *for your encouragement and love.*

I dedicate this work to the memory of my parents, ***Eng. Vasile Brădățan*** *and* ***prof. Veronica Brădățan.***

Liliana

Thanks to the research centres and projects for their support:

- Thanks to the CERNESIM Centre at ICI-UAIC for the infrastructure used to record NMR, FT-IR spectra and X-ray experiments.
- Thanks to the project "Competitiveness Operational Programme POC 2014-2020/448/1/1/Major CD Infrastructures/1/Major CD Infrastructures/ Priority Axis 1/ Investment Priority 1a/, Research Centre with Integrated Techniques for Atmospheric Aerosol Investigation in Romania (RECENT AIR), MySMIS Code: 127324" for the infrastructure used.

Azaheterocycles with condensed nuclei. Synthesis, structure, properties

CONTENTS

INTRODUCTION

Over the years, azaheterocyclic compounds with condensed nuclei have received increased attention due to their multiple applications in various fields such as: pharmaceutical, industrial, or synthetic. The importance of these compounds in the pharmaceutical field is highlighted by the presence of a heterocycle in the structure of various natural and synthetic medicinal drugs. Of this category, the class of nitrogen heterocycles represents the most significant class in nature as a structural unit.

These structures represent the basic skeleton of some categories of medicinal drugs, plastics, dyes and even cosmetics. The presence in the same structural unit of two or more heterocyclic structures could bring new properties. Considering the several aspects presented, the topic chosen for the doctoral thesis was the synthesis, structural characterization, properties and antimicrobial/anticancer testing of new quaternary salts with benzo[*f*]quinolinic skeleton.

Following the tradition of the research laboratory of Prof. univ. dr. Magda Petrovanu, (where I did my doctoral training), I wanted to continue the research whose basis was laid by Prof. univ. dr. Magda Petrovanu (it was a great honor for me to be my professor and a model during the student years) and Prof.univ. dr. Ioan Zugrăvescu.

The synthesis of these cycloimonium salts was carried out starting from quaternized benzo[*f*]quinoline with different halogenated derivatives with increased reactivity, having aliphatic residue or acetophenone skeleton.

An important concern consisted in elucidating the structure of new cycloadducts by spectral analysis and testing them for antimicrobial and anticancer activity.

The doctoral thesis is entitled ***"AZAHETEROCYCLES WITH CONDENSED NUCLEI. SYNTHESIS, STRUCTURE, PROPERTIES"*** and it is structured in two main parts: *literature study* with reference to benzo[*f*]quinoline, structure, synthesis methods, physical and chemical properties, biological properties (antimicrobial, anticancer), optical properties and the part of *personal research* that had as its main purpose the continuation and deepening of research in the field of benzo[*f*]quinoline and derived ylides, both for studying and elucidating some theoretical aspects, as well as for studying and finding some practical applications, especially in the top field of synthetic drugs.

II. PERSONAL RESEARCH

The objectives of the doctoral thesis

The doctoral thesis entitled ***"AZAHETEROCYCLES WITH CONDENSED NUCLEI. SYNTHESIS, STRUCTURE, PROPERTIES "*** had as its main purpose the continuation and deepening of research in the field of benzo[*f*]quinoline and derived ylides, both for the study and elucidation of some theoretical aspects, as well as for the study and finding of practical applications, especially in the top field of synthetic drugs. The research presented in this paper focused on the following operational objectives:

- Synthesis and structural characterization of new quaternary salts with benzo[*f*]quinoline skeleton (K-type);
- Study of dipolar [3+2] cycloaddition reactions of benzo[*f*]quinolinium ylides to symmetrically substituted activated alkenes. Aspects of stereochemistry;
- Study of dipolar [3+2] cycloaddition reactions of benzo[*f*]quinolinium ylides to symmetrically substituted activated alkynes;
- Study of dipolar [3+2] cycloaddition reactions of benzo[*f*]quinolinium ylides to unsymmetrically substituted activated alkynes. Aspects of regiochemistry;
- Obtaining new azaheterocyclic compounds with a condensed structure from the class of benzoquinone-pyrrolo-benzo[*f*]quinoline (type **L**), pyrrolo-benzo[*f*]quinoline (type **M** and **M'**) and tetrahydropyrrolo-benzo[*f*]quinoline (type **N**);
- The structure of the new compounds obtained was proven by modern methods of organic structural analysis: FT-IR, ^{1}H-NMR, ^{13}C-NMR, one- and two-dimensional correlation spectra, high-resolution mass spectrometry (HRMS), X-ray analysis on single crystal;
- The study of the biological properties of some of the new compounds obtained, especially their antibacterial, antifungal, and anticancer activity.

The above objectives can be rationalized according to the scheme below, **Figure II.1.**

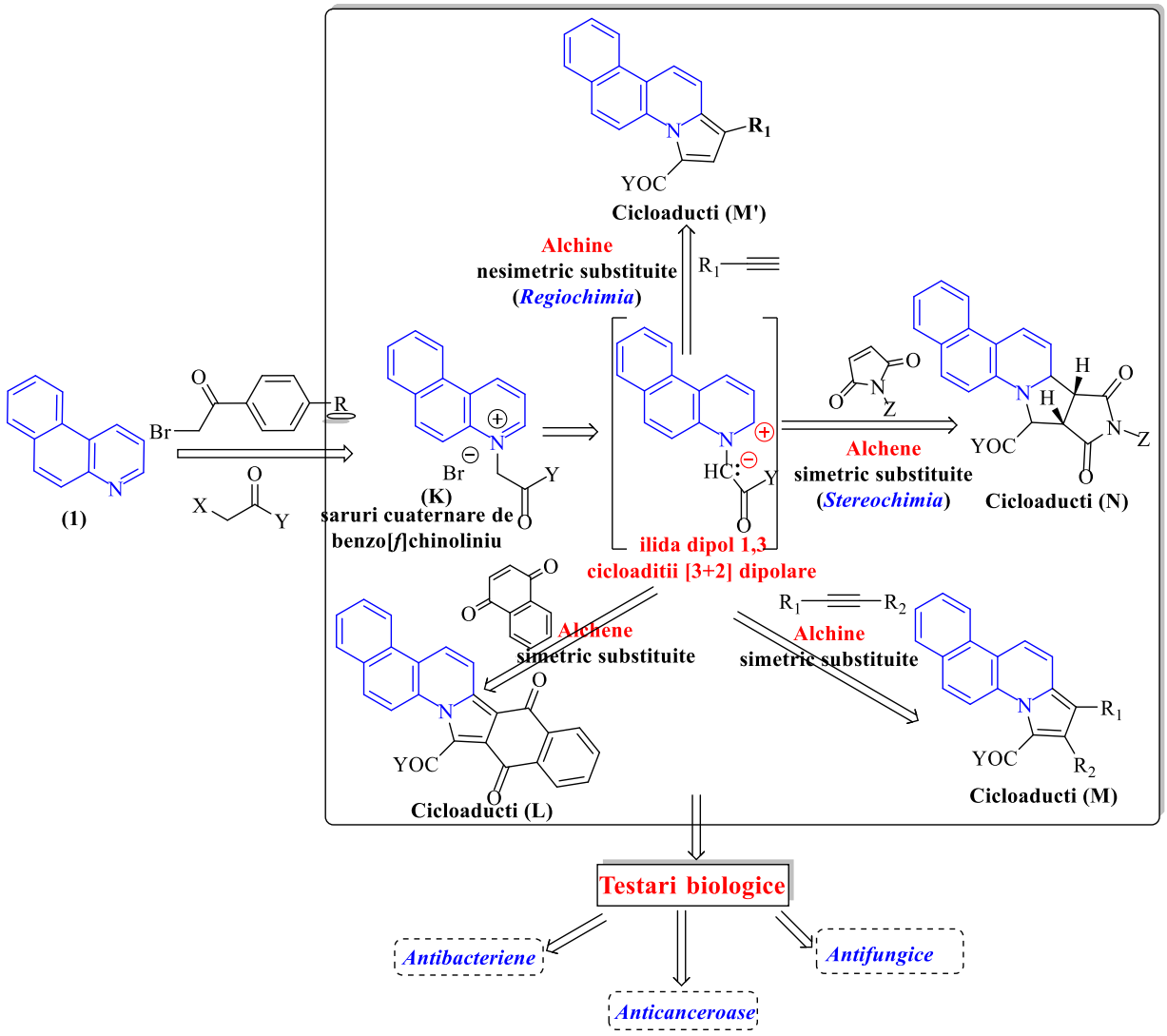

Figure II.1. Logical scheme of the objectives of the doctoral thesis.

II.1. Synthesis of quaternary benzo[f]quinolinium salts

In a first stage of the research, the synthesis of new quaternary benzo[*f*]quinolinium salts with an aliphatic or aromatic residue was carried out, adopting the salt method proposed by Krönke[47], but also improving the methods described in the literature[63,66]. Thus, a series of quaternary benzo[f]quinolinium salts **(4a-d), (5a-i)** were synthesized, starting from benzo[f]quinoline **(1)** and halogenated derivatives with increased reactivity, having an aliphatic residue **(2a -d)**, respectively acetophenone skeleton **(3a-i) (figure II.2)**[68]. The quaternization reactions were carried out using acetone or acetonitrile mixture: toluene (1.5:1 v/v) as solvent, the yields in the desired product being satisfactory (57%-87%).

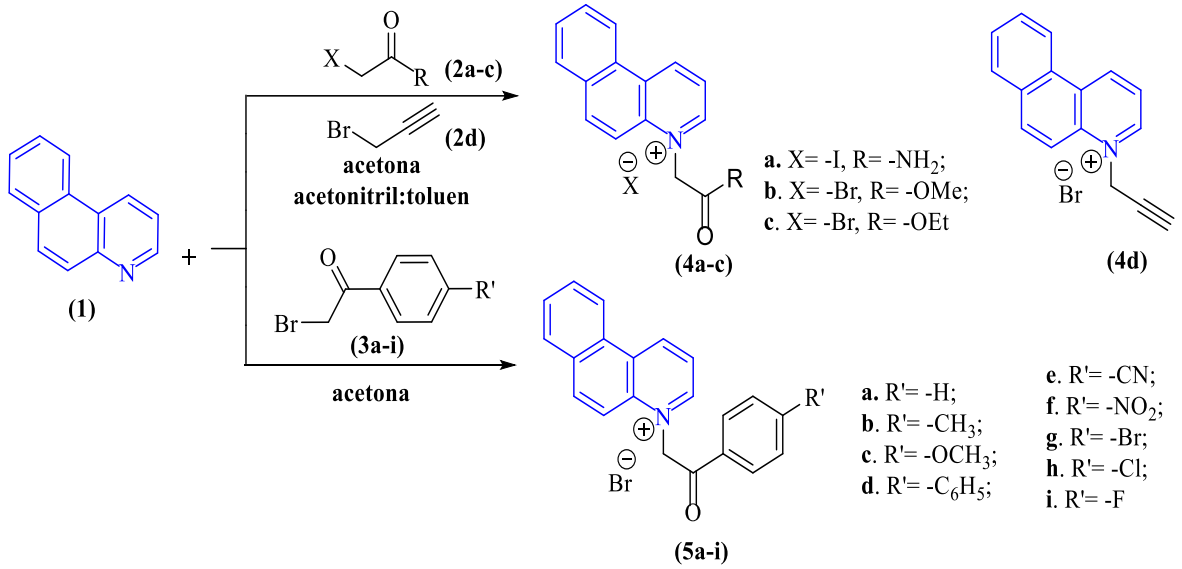

Figure II.2. Synthesis of quaternary benzo[*f*]quinolinium salts with aliphatic residue **(4a-d)**, respectively aromatic skeleton **(5a-i)**.

The quaternary salts with an aliphatic residue **(4a-c)**, respectively the quaternary salt with an aromatic residue **(5c)** were previously reported in the literature[63,66], but within this thesis the efficiency of the chemical synthesis was achieved, which results from the increase in the yield of the desired product, decreasing the amount of solvent used, as well as reducing the working time.

As a representative of the series of quaternary salts with aliphatic residue **(4a-d)**, the benzo[*f*]quinolinium salt **(4d)** with propargylic residue was chosen.

Thus, in the ^{1}H-NMR spectrum of the quaternary salt with a propargylic residue, the most unscreened signal is the one provided by the H-4 proton from the pyridine nucleus which appears at the chemical shift of 10.22 ppm, in the form of a doublet, having a coupling constant J = 8.5 Hz. The next signal is the one provided by the H-2 proton which appears at δ = 9.68 ppm, this descreening being due to its existence in the vicinity of the quaternary nitrogen atom. The correct assignment of these signals was achieved with the help of the HMBC correlation (^{1}H-^{13}C distance correlation), so in this spectrum we can see the distance correlation between the signal of H-2 proton and the C-11 carbon of the methylene residue. The signal of the H-13 acetylenic proton appears as a singlet at a characteristic chemical shift of δ = 4.07 ppm.

The ^{13}C-NMR spectrum of the representatively chosen benzo[*f*]quinolinium salt **(4d)** confirms the proposed structure, thus the most unscreened signal is that provided by the C-2 carbon of the pyridine nucleus (δ = 146.8 ppm), chemical shift which is due to its existence in the vicinity of the quaternary nitrogen atom. The signal of the methylene carbon C-11 appears

at characteristic chemical shifts (δ = 47.8 ppm). The carbon atoms in the triple bond C-12 and C-13 provide signals characteristic of acetylenic carbon atoms (δ = 75.8 ppm and δ = 81.6 ppm, respectively). The other remaining signals in the ^{1}H-NMR and ^{13}C-NMR spectra are also in accordance with the proposed structure.

Table II.1 shows the main absorption and deformation bands characteristic of the representatively chosen quaternary benzo[*f*]quinolinium salt **(4d).** Thus, the most important absorption bands are provided by the vibration of the alkyne C-H bond, as well as the vibration of the alkyne bond $C{\equiv}C$ which appear at the wave numbers 3149 cm^{-1} and 2117 cm^{-1}, respectively, and have an average intensity.

Table II.1 The main vibration (ν) and deformation (δ) bands of the quaternary salt **4d**.

Wave number (ν) (cm^{-1})	**Type of bonding/vibration**
3149	νC-Haromatic, νC-Halkyne
2894	$\nu_{C\text{-}Haliphatic}$
2117	$\nu_{C\equiv C}$
1602, 1511	$\nu_{C=Caromatic}$; $\nu_{C=Naromatic}$
1424	$\delta_{Csp3\text{-}H}$
1346-1235	$\delta_{Csp2\text{-}Haromatic}$
807, 750	$\delta_{C\text{-}H}$

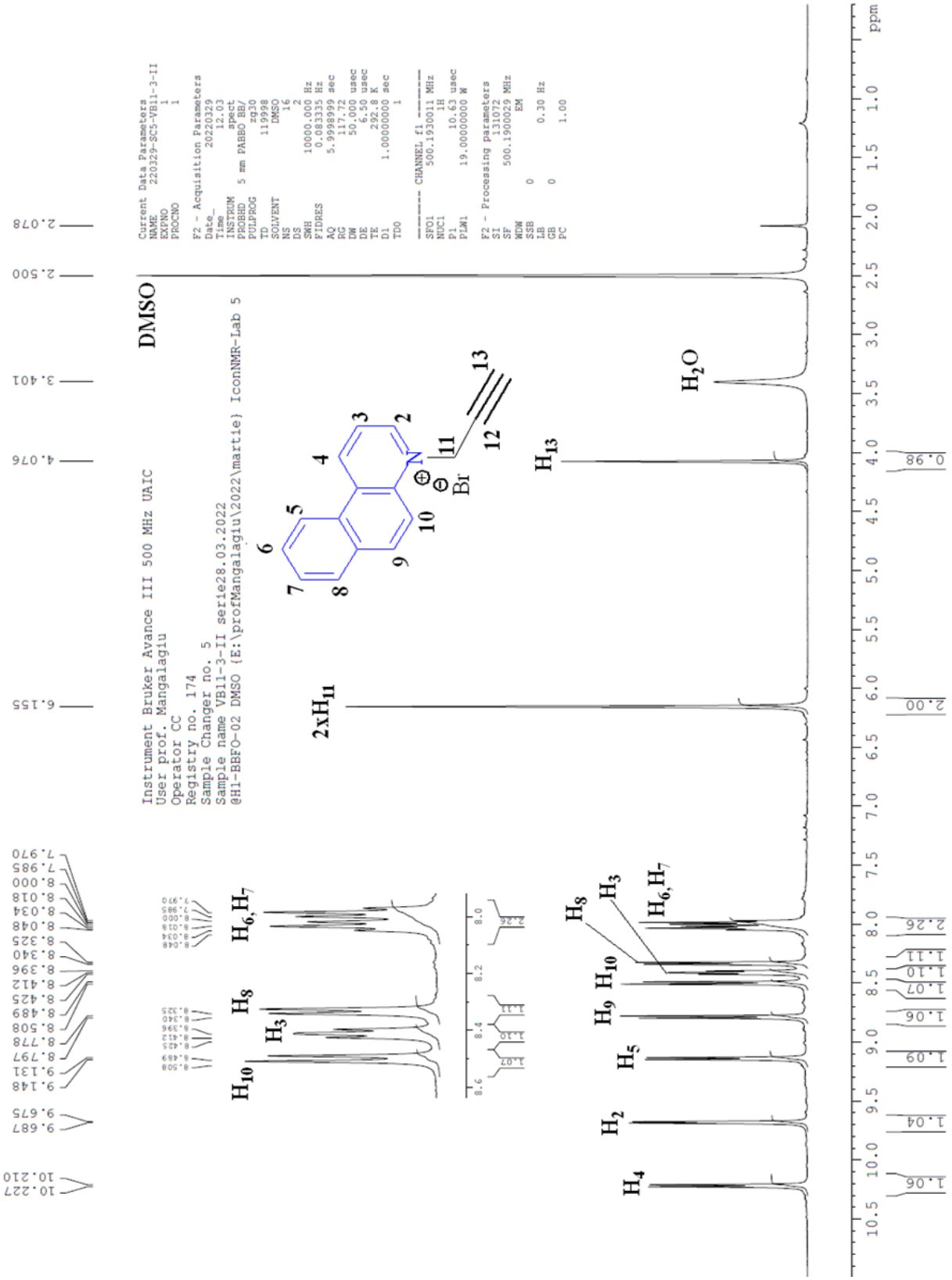

Figura II.3. ^{1}H-NMR spectrum of 4-(prop-2-in-1-yl) benzo[*f*]quinolin-4-ium bromide **(4d)**.

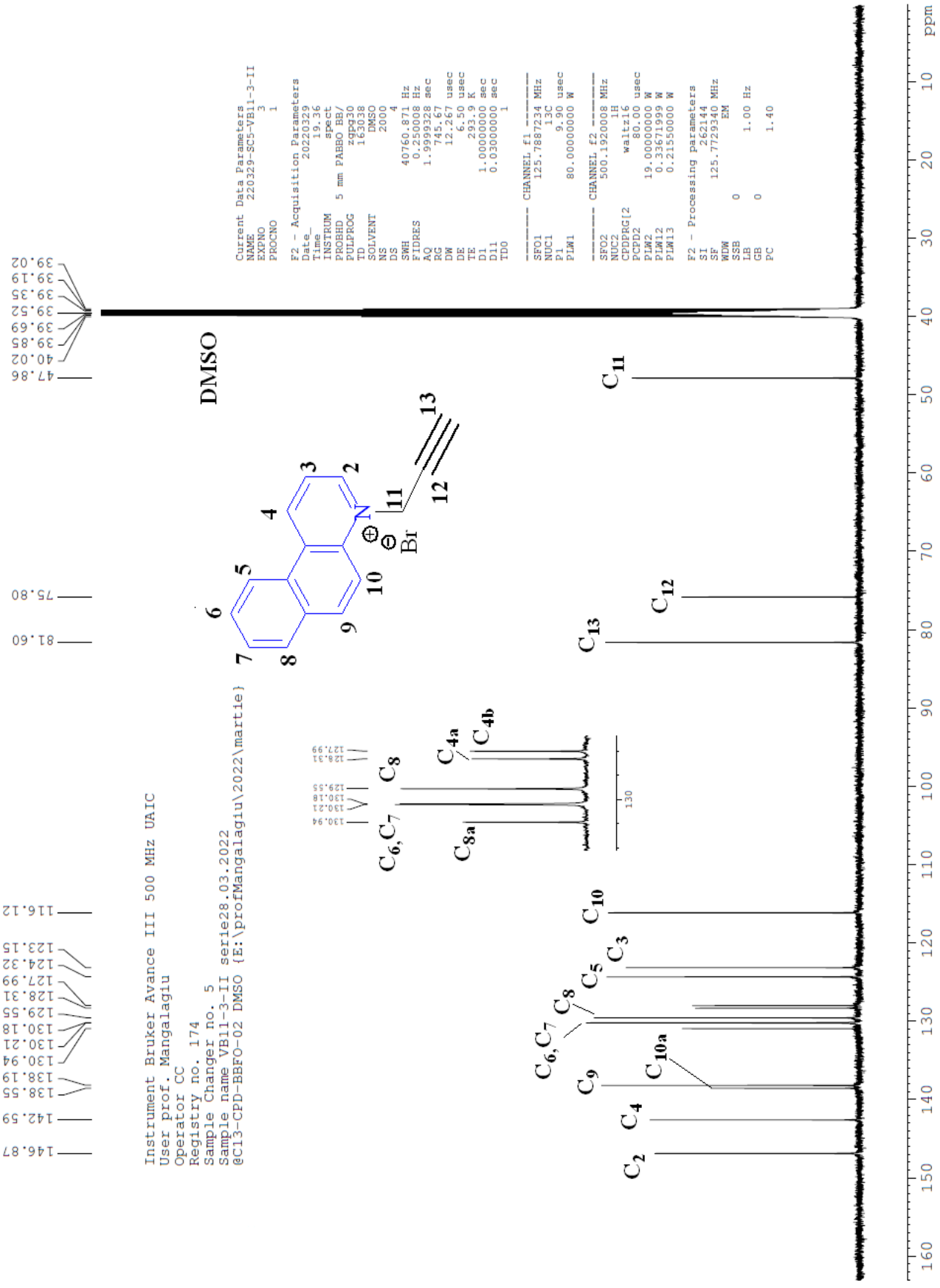

Figura II.5. ^{13}C-NMR spectrum of 4-(prop-2-in-1-yl) benzo[*f*]quinolin-4-ium bromide **(4d)**.

From the series of nine quaternary benzo[*f*]quinolinium salts with an aromatic skeleton **(5a-i),** two cycloimonium salts **(5f)** having a nitro group as a substituent in *para* to the aromatic nucleus, respectively **(5g)** having as substituent in *para* a halogen atom, namely bromine.

In the IR spectrum of the quaternary salt with a *p*-nitro residue **(5f) (figure II.10)**, the most important absorption bands are provided by the vibration of the aromatic, respectively aliphatic C-H bond that appear at the wave numbers 3032 cm^{-1} and 2963 cm^{-1}, respectively.The nitro group is highlighted by two characteristic bands that appear at wave numbers 1520 cm^{-1} (corresponding to the asymmetric valence vibration of the N-O bond ($\nu N\text{-}O_{asim}$)), respectively 1349 cm^{-1} ($\nu N\text{-}O_{sim}$). The band characteristic of the carbonyl group appears at 1717 cm^{-1} ($\nu C{=}O$).

In the IR spectrum of the quaternary salt with *p*-bromo residue **(5g) (figure II.11)** the most important absorption bands are provided by the vibration of the carbonyl bond(1696cm^{-1}) as well as the aromatic C-H bonds (3018 cm^{-1}), respectively aliphatic (2911 cm^{-1}).

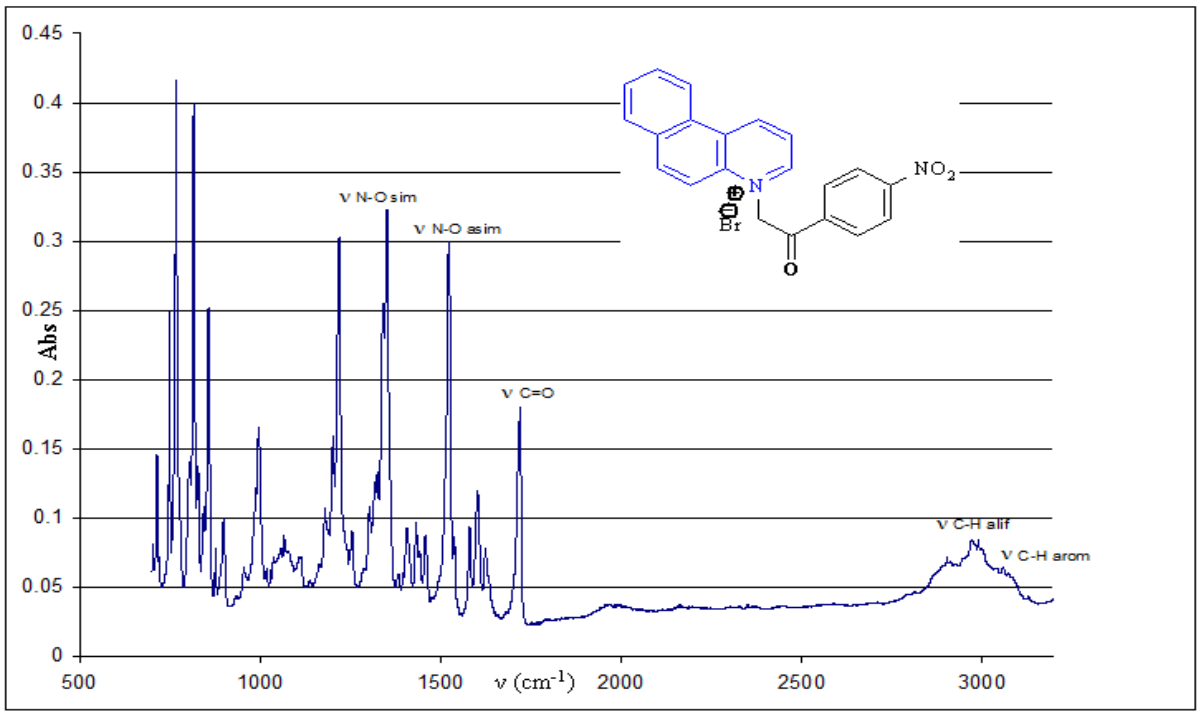

Figure II.10. IR spectrum of 1-(4-nitrophenacyl) benzo[*f*]quinolinium bromide **(5f)**.

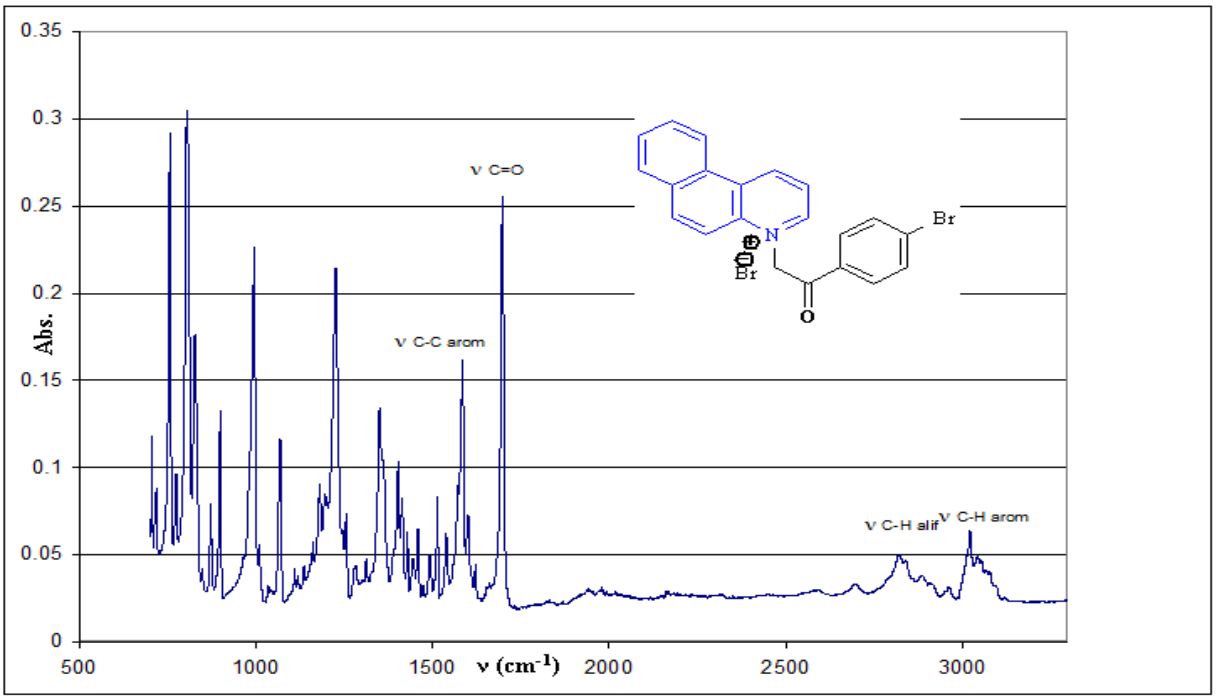

Figure II.11. IR spectrum of 1-(4-bromophenacyl) benzo[*f*]quinolinium bromide **(5g)**.

Considering what is presented in this sub-chapter, the following conclusions can be formulated:

- a series of quaternary benzo[*f*]quinolinium salts with an aliphatic residue (4 cycloimonium salts) and with aromatic skeleton (9 cycloimonium salts), respectively were synthesized;

II.2. Synthesis of new pyrrolo-benzo[f]quinoline derivatives and tetrahydropyrrolo-benzo[f]quinoline derivatives

II.2.1.1 Dipolar [3+2] cycloaddition reactions with 1,4-naphthoquinone

Part of the quaternary benzo[*f*]quinolinium salts, previously synthesized, were subjected to dipolar [3+2] cycloaddition reactions to synthesize new compounds with pyrrolo-benzo[*f*]quinolinic structure. Thus, by the reaction of quaternary salts with aliphatic residue **(4a-c)** or with an aromatic residue respectively **(5 d, h, i)** with a symmetrically substituted cyclic alkene dipolarophile, namely 1,4-naphthoquinone **(6),** in chloroform using triethylamine as a base, the corresponding cycloadducts with pyrrolo-benzo[*f*]quinoline structure **(7a-f)** were obtained, with satisfactory product yields (42%-62%) **(figure II.13)** [69]

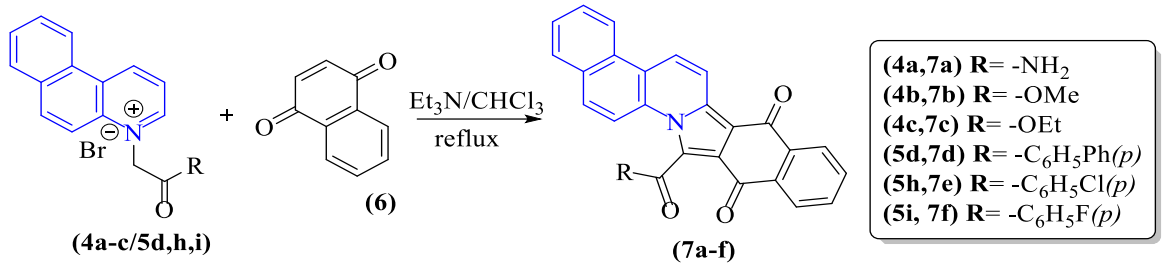

Figure II.13. Synthesis of cycloadducts with pyrrolo-benzo[*f*]quinoline structure **(7a-f)**.

The mechanism of these dipolar [3+2] cycloaddition reactions consists in the *in situ* generation of ylides (**8a-c/9d, h, i)** in the presence of triethylamine from the corresponding quaternary salts **(4a-c/5d,h,i).** They react in the form of dipole-1,3 **(B)** with 1,4-naphthoquinone **(6),** used as a symmetrically substituted cyclic alkene, thus obtaining non-isolation tetrahydropyrrolo-benzo[*f*]quinolinic derivative intermediates **(C)** which, after an oxidative dehydrogenation process, lead to the formation of stable cycloadducts **(7a-f)** with a fully aromatized structure **(figure II.14).**

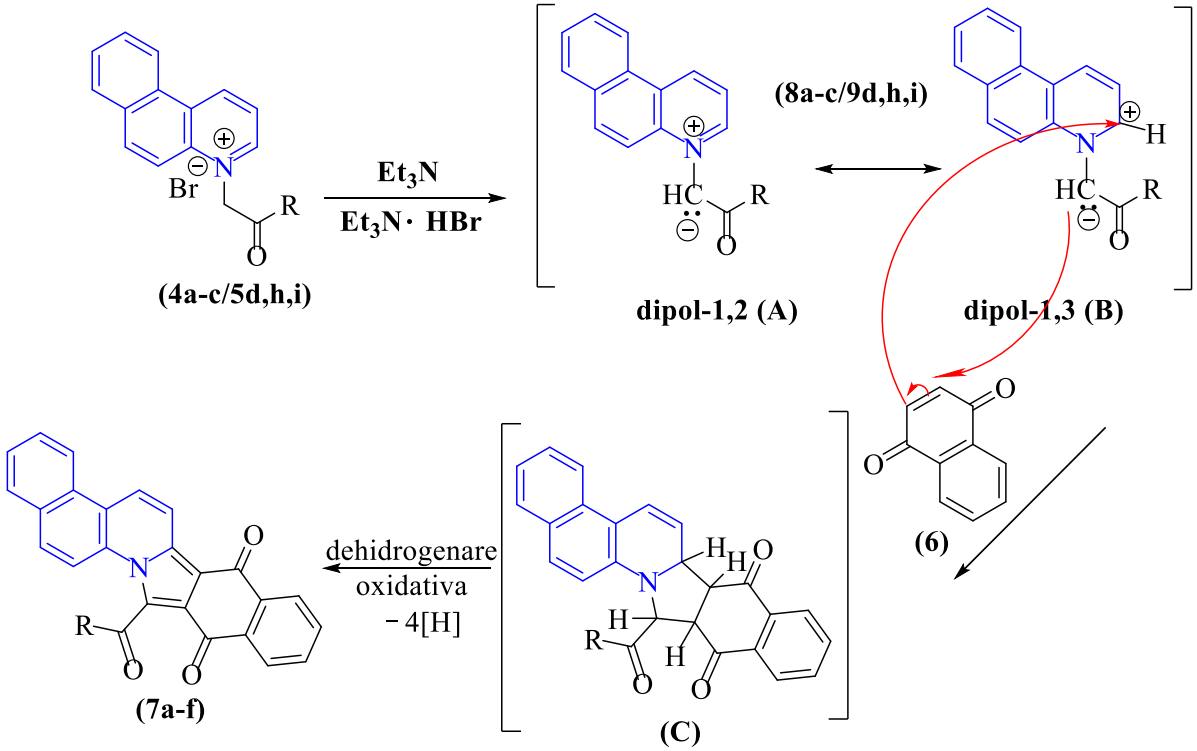

Figure II.14. Synthesis mechanism of pyrrolo-benzo[*f*]quinolinic cycloadducts **(7a-f)**.

The structure of the new pyrrolo-benzo[*f*]quinolinic cycloadducts **(7a-f)** was proved by nuclear magnetic resonance spectroscopy (^{1}H-, ^{13}C -NMR and two-dimensional 2D-COSY, HMQC, HMBC spectra), infrared spectroscopy (FT-IR spectra), mass spectrometry (HRMS spectra), as well as single crystal X-rays (for compound **7c**).

From the series of six new cycloadducts with pyrrolo-benzo[*f*]quinoline structure**(7a-f)**, the compound with *p*-phenyl residue **(7d)** was chosen as representative. The solubilization of the compound for recording the NMR spectra was carried out in deuterated chloroform also using a few drops of deuterated TFA (trifluoroacetic acid) because the compound is not totally soluble in chloroform.

In the IR spectrum of the derivative with pyrrolo-benzo[*f*]quinoline structure **(7d),** the most important absorption bands are provided by the vibration of the aromatic and aliphatic C-H bond respectively that appear at the wave numbers 2991 cm^{-1} and 2889 cm^{-1}, respectively **(figure II.18)**. The absorption band characteristic of the ketone carbonyl group (from the acetophenonic residue) appears at 1661 cm^{-1} ($\nu_{C=Oacetophene}$). Ketonic carbonyl groups from the naphthoquinone residue appear at lower wave numbers 1633 cm^{-1} and 1599 cm^{-1} respectively ($\nu_{C=Onaphto}$). In the range 1545-1464 cm^{-1} there appear absorption bands characteristic of the valence vibration of the aromatic C-C bond superimposed with the valence vibrations of the C-N bonds in the pyridinic/pyrrolic nuclei ($\nu_{C\text{-}Carom}$, $\nu_{C\text{-}N\ pyridinic/pyrrolic}$) (**figure II.18**).

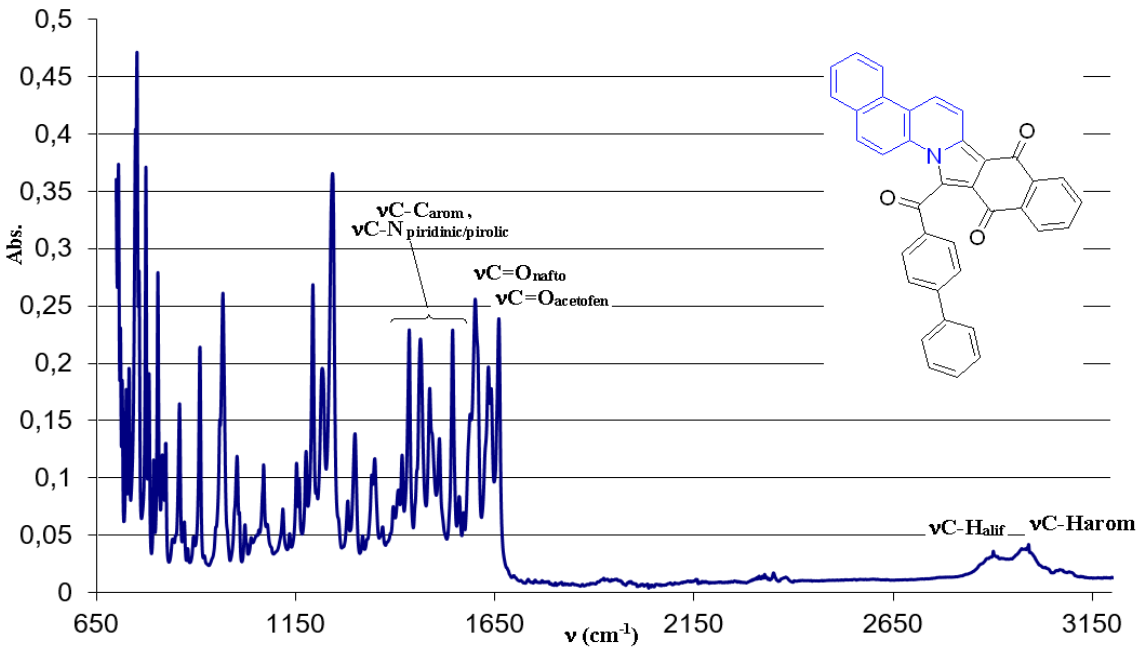

Figure II.18. IR spectrum of 15-([1,1'-biphenyl]-4-carbonyl)benzo[*f*]benzo[5,6]isoindolo[2,1-a]quinoline-9,14-dione **(7d)**.

Single crystal X-ray studies revealed that the derivative with pyrrolo-benzo[*f*]quinoline structure **(7c)** crystallizes in an anhydrous form, the asymmetric unit being represented by one molecule **(figure II.19-a).** The cell is described by a triclinic system with a *P*-1 symmetry group, having the parameters a = 6.9814 Å, b = 11.3238 Å, c = 13.1202 Å, α = 78.690°, β = 75.608°, γ = 81.707°, occupying a total volume of 980.18 Å3, specific for 2 compound

molecules. Typical intermolecular interactions are not present for this compound. When packed **(figure II.19-c),** the array of molecules is distributed in a planar configuration with respect to each other, except for the ethyl carboxylic group.

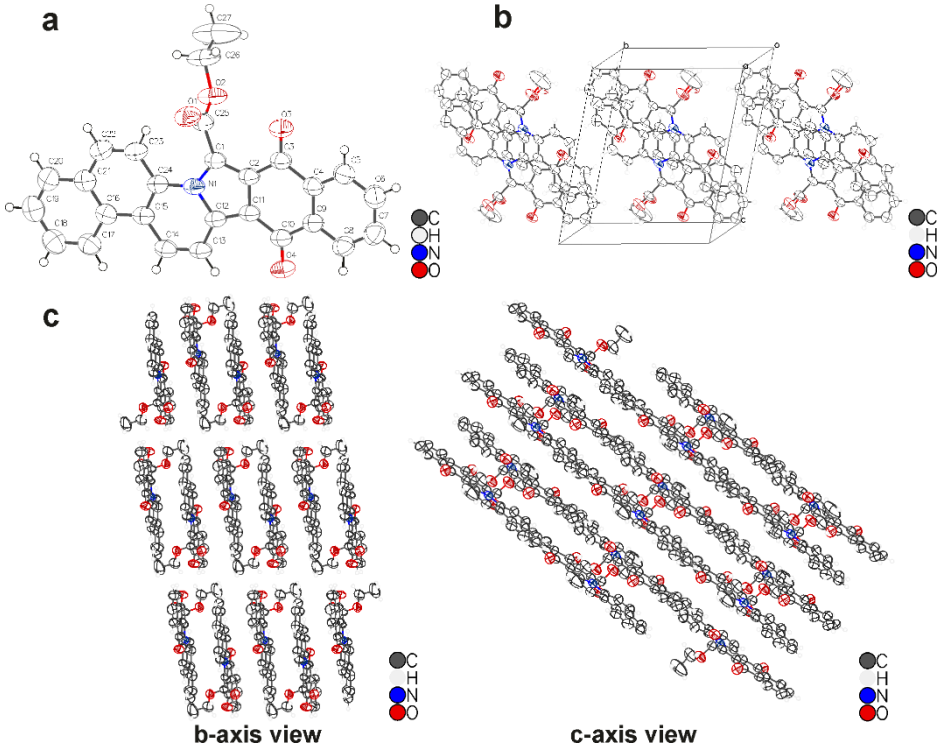

Figure II.19. Asymmetric unit **(a);** elementary cell **(b);** packing of the molecules in the 2x2x2 crystal **(c)** for compound **(7c).** *Hydrogen atoms are highlighted in figure **(a)** only.

The following table highlights the main structural information related to the X-ray diffraction analysis of the cycloadduct **(7c).** Orange coloured single crystals were obtained by slow crystallization using absolute ethanol. In **Appendix 1**, the data from *checkCIF files* of the discussed cycloadduct **(7c)** are presented.

Table II.2 Crystallographic data and refined structure information of ethyl 9,14–dioxo–9,14–dihydrobenzo[*f*]benzo[5,6] isoindolo[2,1–a]quinoline–15–carboxylate **(7c)**.

Molecular formula	**$C_{27}H_{17}NO_4$**	**Crystal size /mm^3**	**0.04 × 0.06 × 0.78**
Molecular mass	419.42	**Radiation**	CuKα (λ = 1.54184)
Temperature/K	293(2)	**2Θ range for data collection/°**	3.528 to 70.862
The crystalline system	triclinic	**Index ranges**	-5 ≤ h ≤ -8, -13 ≤ k ≤ 13, -16 ≤ l ≤ 15
Space group	*P*-1	**Reflections collected**	7201
Cell lengths (Å)	a=6.9814(4) b= 11.3238(8)	**Independent reflections**	3685 [R_{int} = 0.0149, R_{sigma} = 0.0253]

	c= 13.1202(9)		
Cell angles /°	α= 78.690(6) β= 75.608(6) γ= 81.707(5)	**Data/restraints/parameters**	3685/6/290
Cell volume /Å^3	980.18(12)	**Goodness-of-fit on F^2**	1.029
Z	2	**Final R indexes [I>=2σ (I)]**	R_1 = 0.0453, wR_2 = 0.1193
ρ_{calc}g/cm^3	1.421	**Final R indexes [all data]**	R_1 = 0.0637, wR_2 = 0.1353
μ/mm^{-1}	0.781	**Largest diff. peak/hole / e Å^{-3}**	0.219/-0.187
F(000)	436		

II.2.1.2 Dipolar [3+2] cycloaddition reactions with N-phenylmaleinimide (NFMI) and N-ethylmaleinimide (NEMI) respectively

To diversify the newly synthesized compounds with a benzo[*f*]quinolinium skeleton, new symmetrically substituted cyclic alkenes (NFMI and NEMI) were chosen, as well as in order to study the [3+2] dipolar cycloaddition reactions of benzo[*f*]quinolinium ylides with these alkenes, reactions involving aspects of stereochemistry.

In the first phase, to study the stereochemistry aspects mentioned above, we treated quaternary benzo[f]quinolinium salts of type **(4a-d and 5a-i)** with *N*-ethylmaleinimide (NEMI) **(10)** and *N*- phenylmaleimide (NFMI) respectively **(11)** into 1,2-butylene oxide **(12).** Surprisingly, regardless of the conditions used, our attempts were not successful except for the case of the reaction of the salt **(5f),** otherwise they led to non-isolable degradation products. To date we do not have a coherent explanation for this, but our efforts will continue both to realize these reactions and to find pertinent explanations where the reactions do not occur.

Thus, by treating the quaternary benzo[*f*]quinolinium salt with a *p*-nitro residue **(5f)** with *N*-ethylmaleinimide (NEMI) **(10)** and *N*-phenylmaleinimide (NFMI) **(11)** in 1,2-butylene oxide **(12),** used both as a solvent and as a base, cycloadducts with tetrahydro-pyrrolobenzo[*f*]quinoline structure **(13a-b)** were obtained **(figure II.20).**

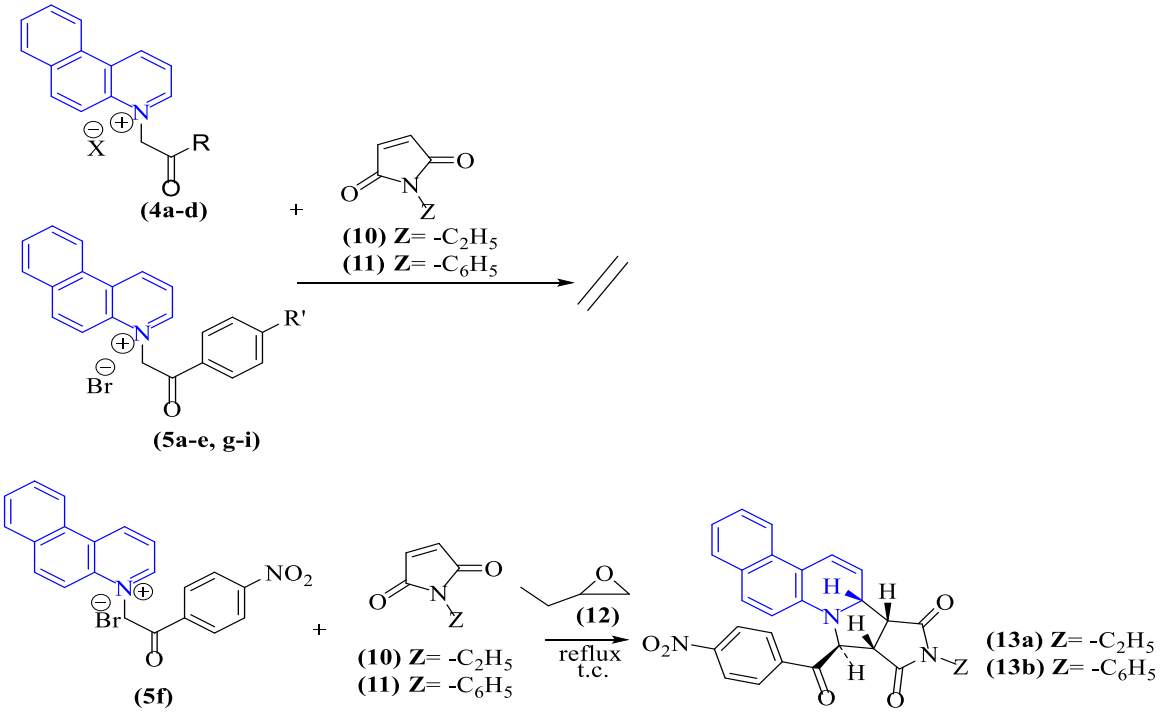

Figure II.20. Synthesis of cycloadducts with tetrahydro-pyrrolo benzo[*f*]quinoline structure**(13a-b)**.

Based on specialized literature[67], the mechanism of cycloaddition reactions involves, in a first stage, the attack of the halide anion from the quaternary ammonium salt **(5f)** on a carbon atom from the strained ring of 1,2-butylene oxide **(12),** with the opening of the ring and formation of an alkoxide intermediate **(14).** It takes the proton from the methylene group of the quaternary benzo[f]quinolinium salt **(5f),** thus generating the ylide, dipol-1,2 **(A),** and 2-bromobutan-1-ol **(15).** The ylide thus generated in the form of dipole-1,3 **(B)** reacts through a concerted mechanism with the dipolarophile (NEMI **(10)** or NFMI **(11)**), forming cycloadducts with the structure tetrahydro-pyrrolo-benzo[*f*] quinoline **(13a-b) (figure II.21).**

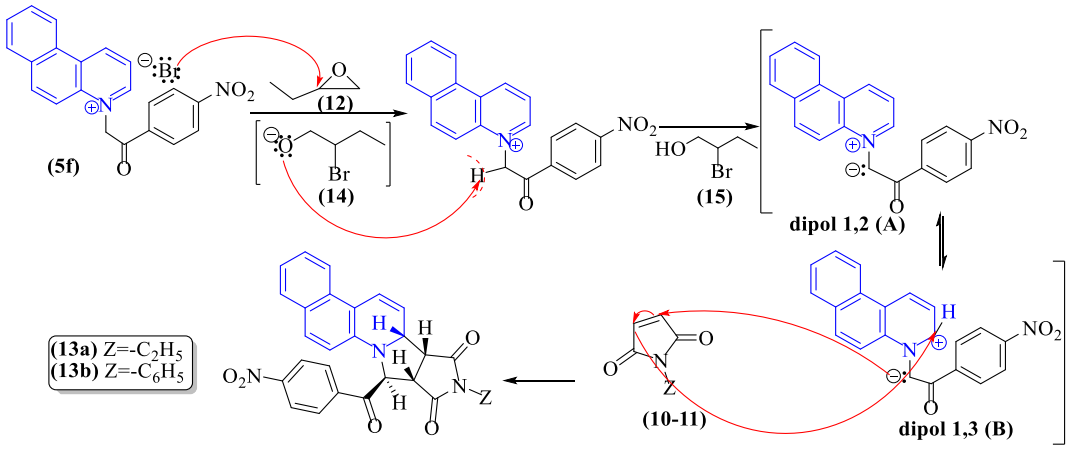

Figure II.21. The proposed mechanism for the synthesis of cycloadducts with tetrahydro-pyrrolo benzo[*f*]quinoline structure **(13a-b)**.

From the series of two new cycloadducts with tetrahydropyrrolo-benzo[*f*]quinolinic structure **(13a-b),** compound **(13b)** was chosen as representative.

Table II.3 shows the main absorption and deformation bands characteristic of the cycloadduct with benzo[*f*]quinoline skeleton as representative **(13b).** Thus, the most important absorption bands are provided by the vibration of the carbonyl bonds from the acetophenone residue and from the pyrrolidinone residue respectively that appear at wave numbers 1701cm^{-1} ($\nu_{C=Oacetophen}$) and 1597 cm^{-1} ($\nu_{C=Opyrrolidinone}$) respectively. The nitro group is highlighted by two characteristic bands that appear at wave numbers 1525 cm^{-1} (corresponding to the asymmetric valence vibration of the N-O bond ($\nu_{N-Oasym}$)) respectively 1342 cm^{-1} (ν_{N-Osym}).

Table II.3 The main vibration (ν) and deformation (δ) bands of cycloadduct **13b**.

Wave number (ν) (cm^{-1})	**Type of bond/vibration**
3105	$\nu_{C-Haromatic}$
2930	$\nu_{C-Halifatic}$
1701	$\nu_{C=Oacetofen}$
1597	$\nu_{C=Opirolidinonă}$
1525	$\nu_{N-Oasim}$
1342	ν_{N-Osim}
1183-997	$\delta_{Csp2-Haromatic}$
845, 743, 697	δ_{C-H}

II.2.2 Dipolar [3+2] cycloaddition reactions of benzo[*f*]quinolinium ylides to symmetrically/unsymmetrically substituted activated alkynes

According to literature data, a class of dipolarophiles often used in dipolar [3+2] cycloaddition reactions is alkynes, since Z-substituted alkynes are dipolarophiles with increased reactivity, especially when they are conjugated[54,63,61,66,67].

II.2.2.1 Dipolar [3+2] cycloaddition reactions of benzo[f]quinolinium ylides with methyl acetylenedicarboxylate (DMAD)

According to the previously presented literature data (chapter I.7 of the literature report), the dipolar [3+2] cycloaddition reactions of benzo[*f*]quinolinium ylides with symmetrically substituted activated alkynes constitute an excellent method for obtaining condensed heterocycles with the structure of the pyrrolo-benzo[*f*]quinolinic type. According to data from the literature, using DMAD (methyl acetylenedicarboxylate) as a symmetrically substituted

activated alkyne, by reacting with benzo[*f*]quinolinium ylides, more stable aromatic cycloadducts of the pyrrolo-benzo[*f*]quinolinic[62,63,66,67] type are obtained.

Thus, by the reaction of quaternary benzo[*f*]quinolinium salts with an aliphatic residue **(4a-d)** with methyl acetylenedicarboxylate (DMAD) **(16),** in 1,2-butylene oxide **(12),** used both as a solvent and as an acceptor of HBr, the corresponding pyrrolo-benzo[*f*]quinoline structure cycloadducts **(17a-d)** were obtained, with satisfactory yields (45%-70%) (**figure II.25**)[69].

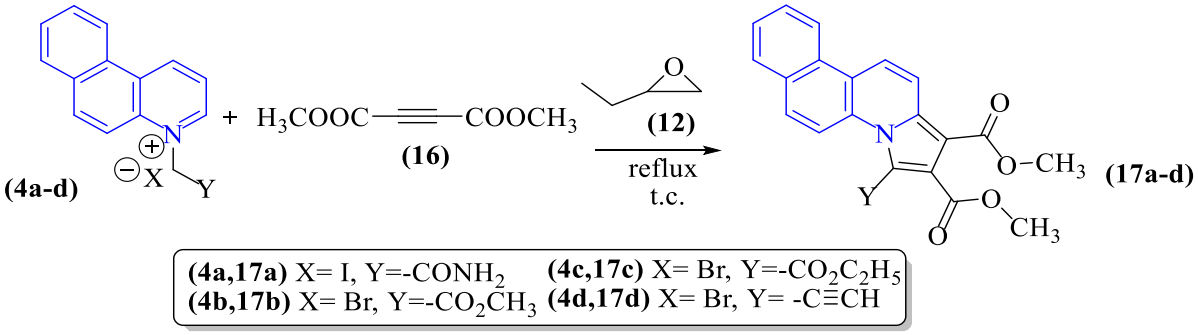

Figure II.25. Synthesis of cycloadducts with pyrrolo-benzo[*f*]quinoline structure **(17a-d)**.

Studying the literature[67] the mechanism of [3+2] dipolar cycloaddition reactions with DMAD involves:

- attack of the halogenide anion of the quaternary ammonium salts **(4a-d)** on a carbon atom of the strained 1,2-butyleneoxide ring **(12),** resulting in ring opening and formation of an alkoxide intermediate **(14');**
- the intermediate **(14)** takes up the proton from the methylene gupylation of the quaternary benzo[f]quinolinium salts (4a-d), thus generating the ilides, dipol-1,2 **(A')**, and 2-bromobutan-1-ol **(15)** or 2-iodobutan-1-ol **(15')**;
- the ylides generated *in situ*, in the form of dipole-1,3 **(B')** react through a concerted mechanism with the dipolarophile DMAD **(16),** forming cycloadducts with a dihydro-pyrrolo-benzo[f]quinoline structure **(C)** which are unstable and through an oxidative dehydrogenation process will pass into fully flavored compounds **(17a-d)** (**figure II.26**).

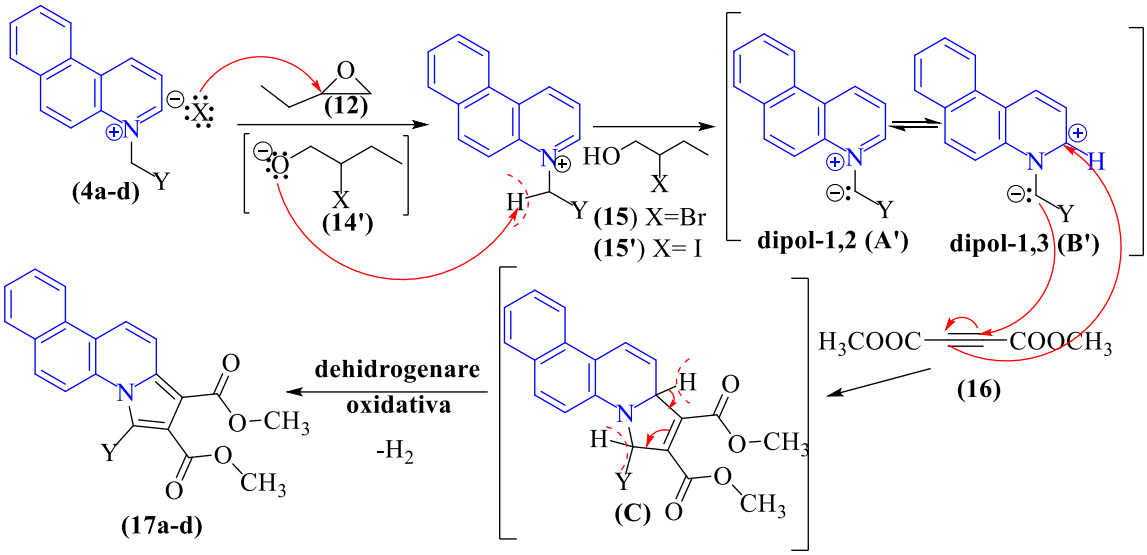

Figure II.26. The proposed mechanism for the synthesis of cycloadducts with pyrrolo-benzo[*f*]quinoline structure **(17a-d)**.

From the new series of four cycloadducts with pyrrolo-benzo[*f*]quinoline structure **(17a-d)** the compound with the Y carboethoxy residue was chosen as representative **(17c)**.

In the IR spectrum of the derivative with pyrrolo-benzo[*f*]quinoline structure **(17c),** the most important absorption bands are provided by the vibration of the three ester carbonyl groups appearing at characteristic wave numbers 1736 cm^{-1}, 1716 cm^{-1}, 1693 cm^{-1}, respectively ($\nu_{C=Oester}$) **(figure II.30)**. In the range 1543-1361 cm^{-1} absorption bands appear, which are characteristic of the valence vibration of the aromatic C-C bond superimposed with the valence vibrations of the C-N bonds in the pyridinic/pyrrolic nuclei ($\nu_{C-Carom}$, $\nu_{C-N\ pyridinic/pyrrolic}$). At wave numbers 1217 cm^{-1} and 1174 cm^{-1} respectively, absorption bands appear that are attributed to the asymmetric and symmetric valence vibrations specific to C-O-C ester groups.

At high wave numbers, absorption bands of medium intensity appear that are characteristic of aromatic C-H and aliphatic C-H bonds, respectively (3001 cm^{-1}, 2921 cm^{-1}, 2847 cm^{-1}).

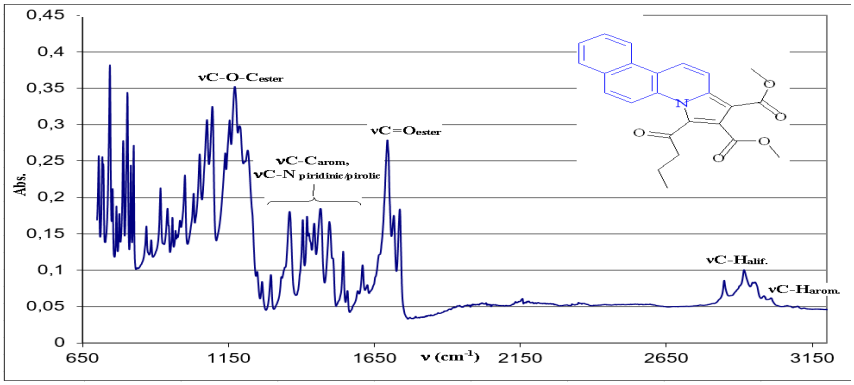

Figure II.30. IR spectrum of 3-ethyl 1,2-dimethyl benzo[*f*]pyrrolo[1,2-a] quinoline-1,2,3-tricarboxylate **(17c).**

II.2.2.2 Dipolar [3+2] cycloaddition reactions of benzo[f]quinolinium ylides with ethyl propiolate. Aspects of regiochemistry

In the research presented in this thesis, the [3+2] dipolar cycloaddition reactions of quaternary aliphatic-restricted benzo[*f*]quinolinium salts (**4a-c)** with ethyl propiolate **(18)** (non-symmetrically substituted activated alkyne) were carried out, in 1,2-butyleneoxide **(12),** used both as solvent and as HBr acceptor, when the corresponding pyrolo-benzo[*f*]quinolinium cycloadducts **(19a-c)** were obtained with satisfactory yields of the desired product (50%-68%) **(Figure II. 33)**[69]. From a regiochemical point of view the meaning of the presented cycloaddition reactions is dictated by the electron factors (pathway I) obtaining a single regioisomer of type A', intermediate generating a dihydro compound **(C')**, unstable, which by oxidative dehydrogenation leads to stable fully aromatized compounds **(19a-c)**, **(figure II.33)**

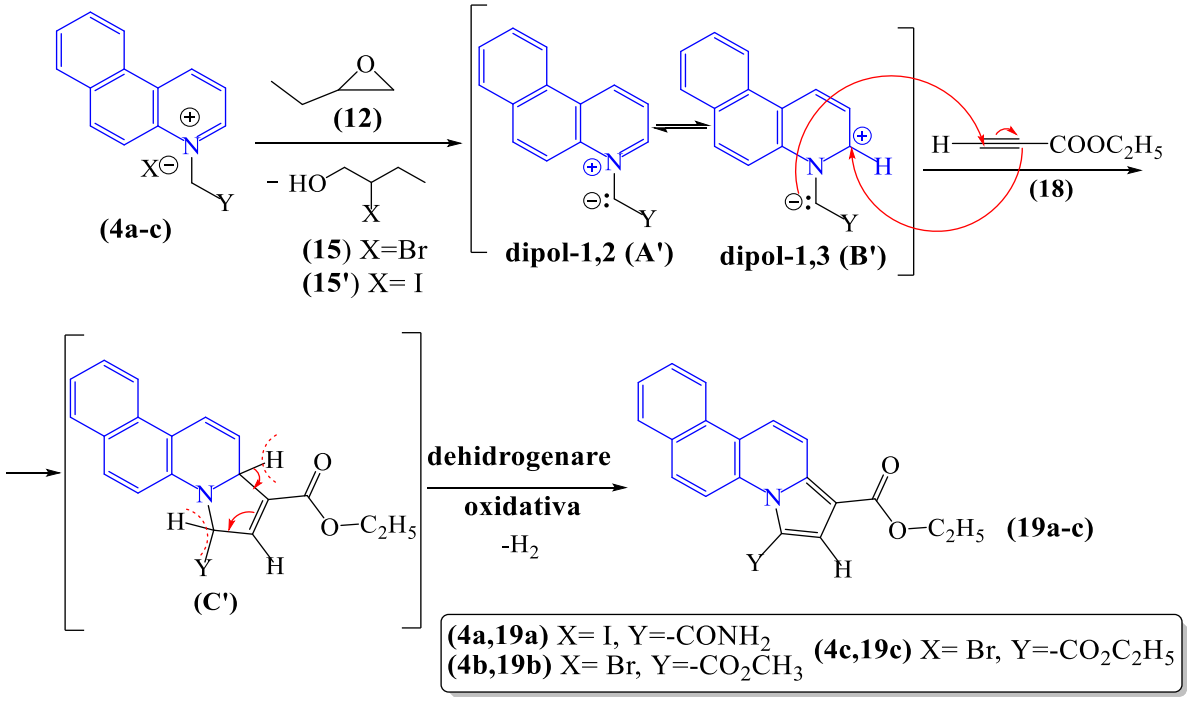

Figure II.33. Synthesis of cycloadducts with pyrrolo-benzo[*f*]quinoline structure **(19a-c)**.

Cycloadducts with pyrrolo-benzo[f]quinoline structure **(19b,c)** were previously reported in the literature in 1977 when they were characterized only by infrared spectroscopy[62], likewise the compound **19a** was previously reported in the literature[63]. In the framework of the current research, the improvement of the working conditions was achieved, which consisted in the use of 1,2-butylene oxide both as a solvent and as a collecting agent for HBr; formely the reactions took place in chloroform using triethylamine as a base, reducing the working time, also achieving an increase in the yield in the desired compound. As representative of the series of three cycloadducts with pyrrolo-benzo[*f*]quinoline structure **(19a-c),** the compound with carbomethoxy residue Y **(19b)** was chosen.

II.3. Biological properties of derivatives with benzo[f]quinoline skeleton

II.3.1. Antimicrobial properties of quaternary benzo[*f*]quinolinium salts and of some cycloadducts with pyrrolo-benzo[*f*]quinolinium structure

The antimicrobial tests of some derivatives with a benzo[*f*]quinolinic skeleton[68] were carried out. Thus, the sensitivity of microorganisms to the investigated substances, quaternary benzo[*f*]quinolinium salts with aliphatic residues **(4a-c)** and aromatic residues **(5a-i),** as well as some cycloadducts with pyrrolo-benzo[*f*]quinolinic structure **(7a-f),** was evaluated based on the diameter of the zone of inhibition, using the Kirby-Bauer agar disk diffusion method, adopted by the Institute for Clinical & Laboratory Standardization (CLSI M07-A11, 2018)[68,74] (**figure II.38**).

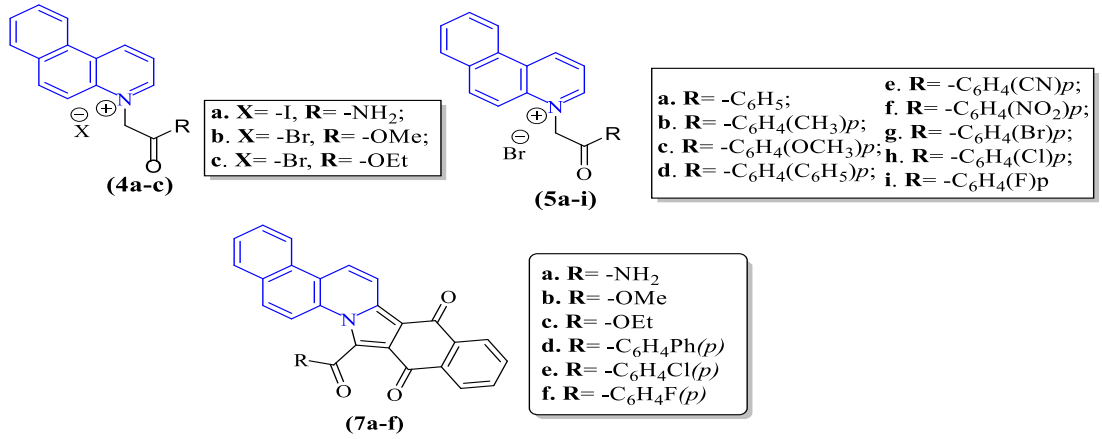

Figure II.38. Structure of quaternary benzo[*f*]quinolinium salts with aliphatic residue **(4a-c)** and aromatic **(5a-i)** respectively, and some cycloadducts with pyrrolo-benzo[*f*]quinolinic structure **(7a-f)** subjected to antimicrobial testing.

The antibacterial activity *in vitro* was evaluated against the Gram-positive bacterium *Staphylococcus aureus* **ATCC 25923** and the Gram-negative bacterium *Escherichia coli* **ATCC 25922**. The antifungal activity *in vitro* was evaluated against the fungus *Candida albicans* **ATCC 10231**. Penicillin (10 IU), carbenicillin (100 μg/mL) and nystatin (500,000 IU) were used as a positive control (C+) for *Staphylococcus aureus*, *Escherichia coli* and *Candida albicans*, respectively. The larger the diameter of the inhibition zones, the more active the compounds are as antimicrobials and antifungals.

Some of the antimicrobial testing results are highlighted in **figures II.39** (tests against *Staphylococcus aureus* **ATCC 25923**), **figure II.40** (tests against *Escherichia coli* **ATCC 25922**), and **figure II.41** (tests against *Candida albicans* **ATCC 10231**), respectively.

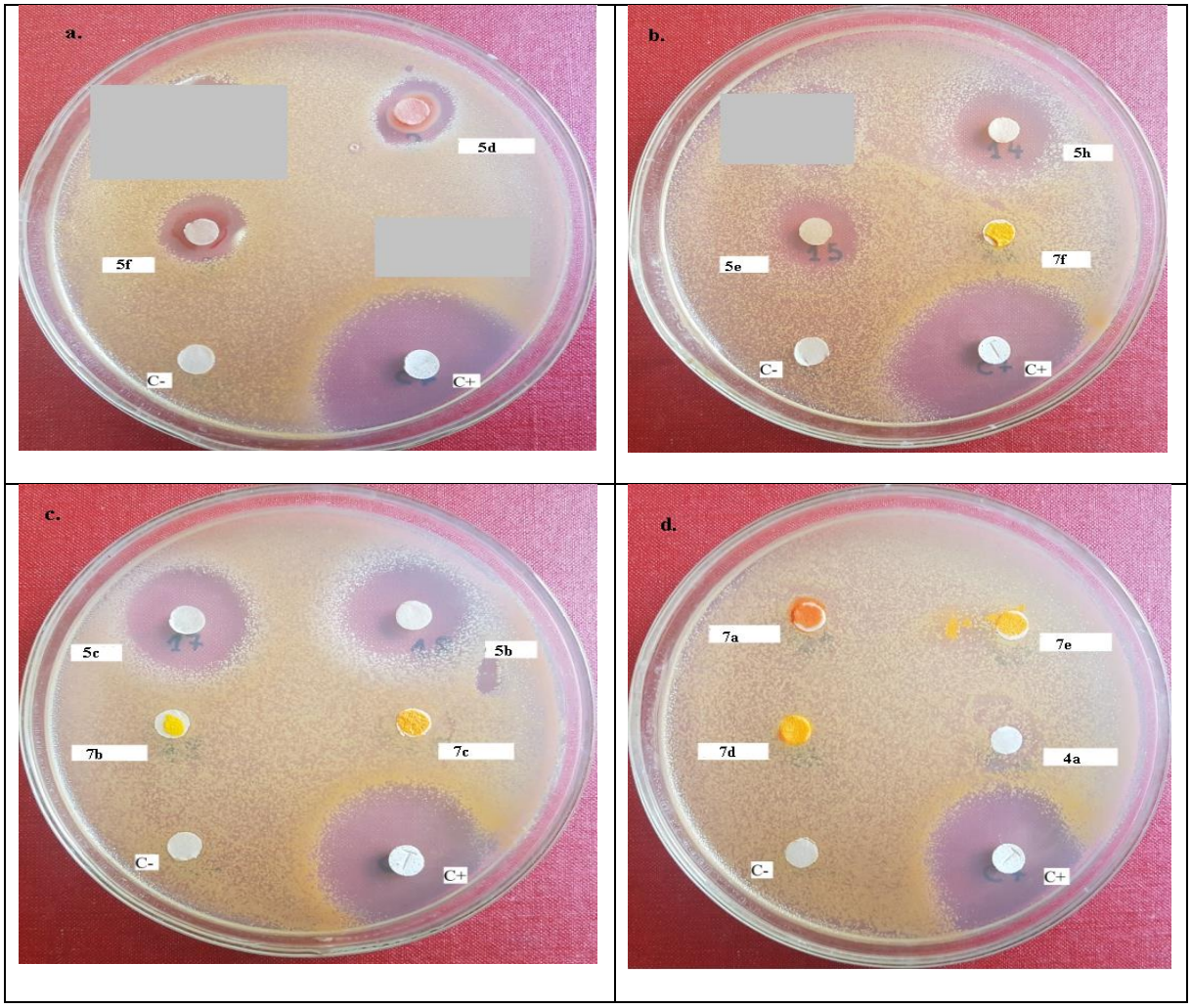

Figure II.39. Testing the antibacterial activity of quaternary salts **5d** and **5f (figure a)**, **5e, 5h (figure b)**, **5b**, **5c (figure c)**, **4a (figure d)** and cycloadducts **7f (figure b)**, **7b, 7c (figure c)**, **7a, 7d, 7e (figure d)** against *Staphylococcus aureus* (C+: positive control, C-: negative control).

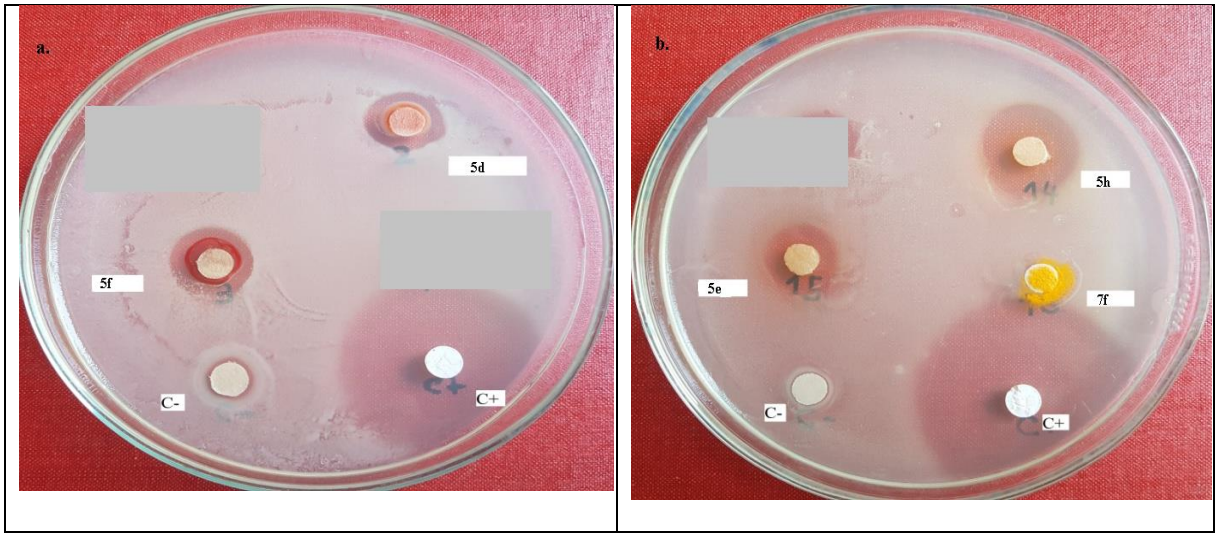

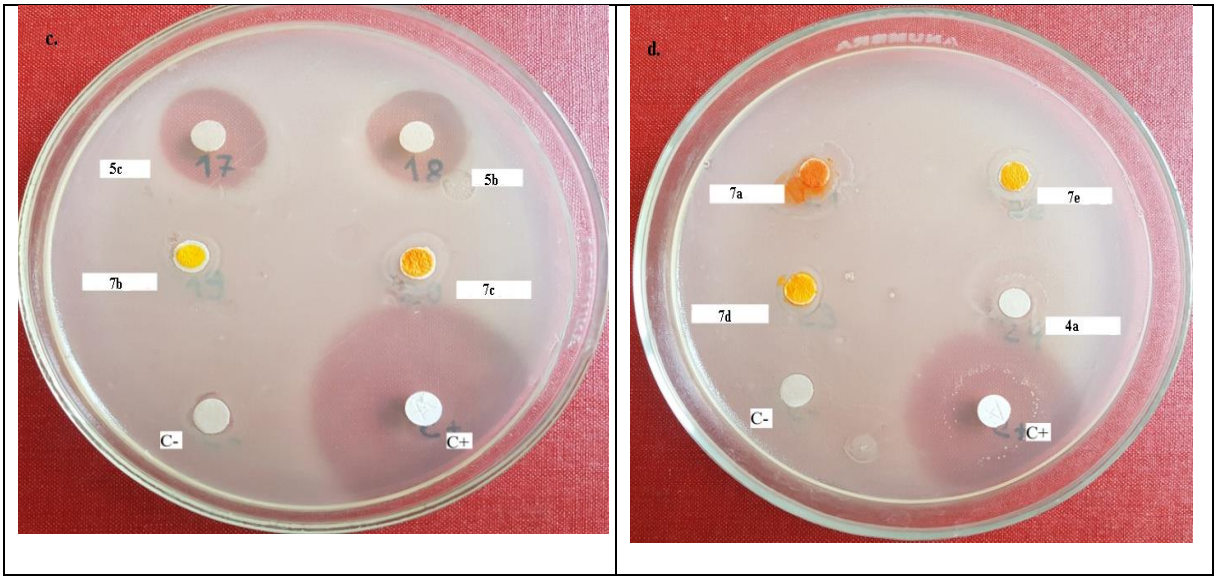

Figure II.40. Testing the antibacterial activity of quaternary salts **5d** and **5f (figure a), 5e, 5h (figure b), 5b, 5c (figure c), 4a (figure d)** and cycloadducts **7f (figure b), 7b, 7c (figure c), 7a, 7d, 7e (figure d)** against *Escherichia coli* (C+: positive control, C-: negative control).

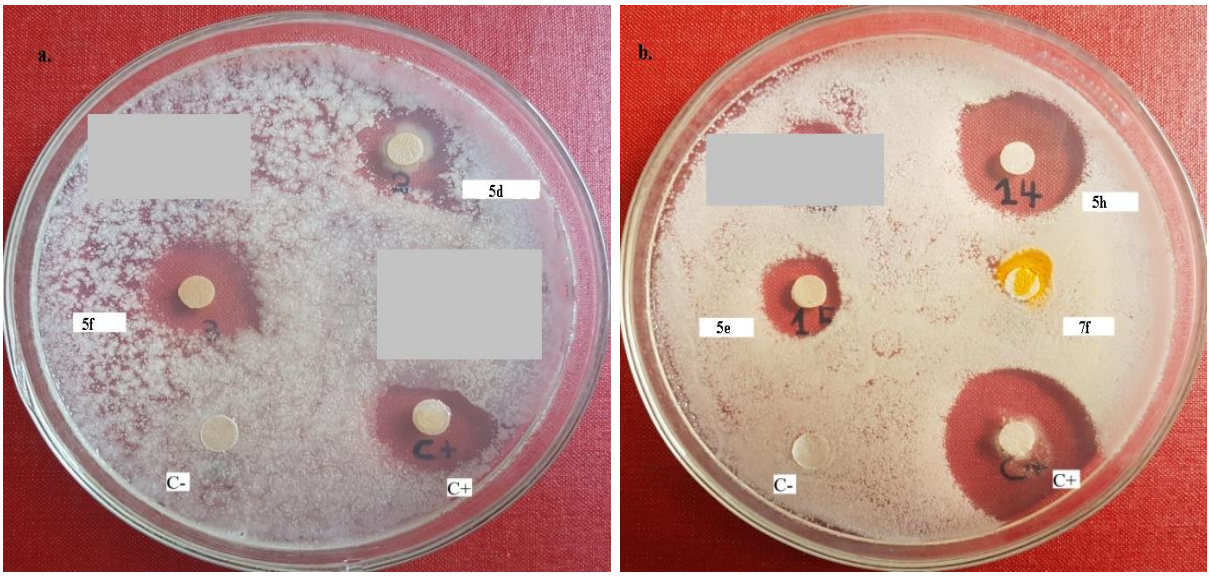

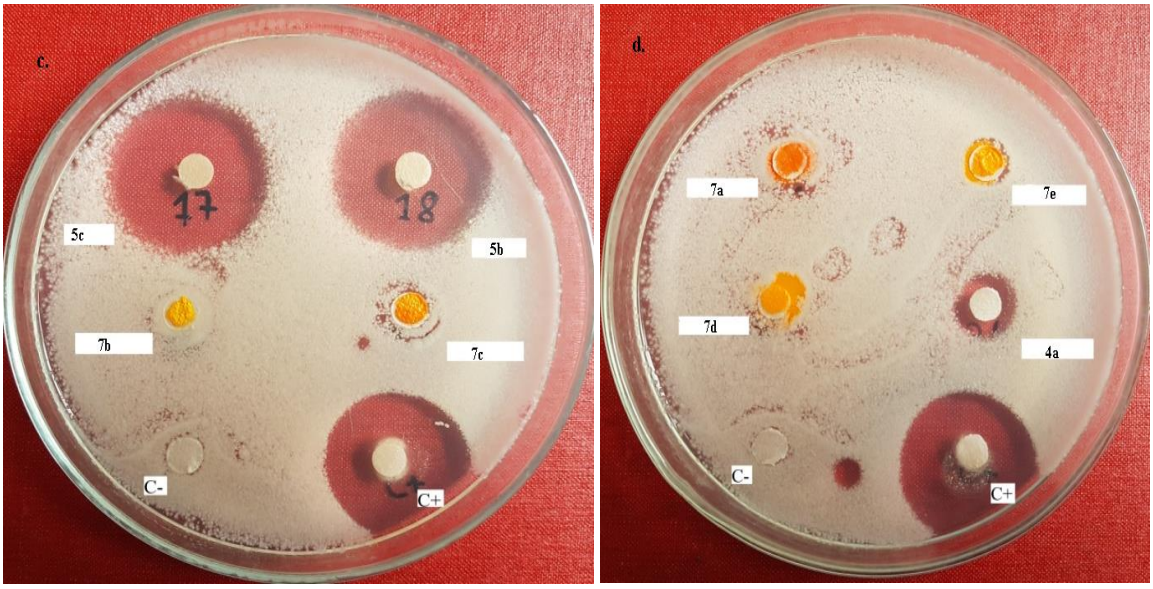

Figure II.41. Testing the antifungal activity of quaternary salts **5d** and **5f (figure a), 5e, 5h (figure b), 5b, 5c (figure c), 4a (figure d)** and cycloadducts **7f (figure b), 7b, 7c (figure c), 7a, 7d, 7e (figure d)** against *Candida albicans* (C+: positive control, C-: negative control).

The results of all compounds with benzo[*f*]quinoline skeleton subjected to antimicrobial testing, expressed as diameters of inhibition zones (mm) are shown in **table II.5**.

Table II.5 Antibacterial and antifungal activity or quaternary benzo[*f*]quinolinium salts with aliphatic residues **(4a-c)** and aromatic residues **(5a-i),** and some cycloadducts with pyrrolo-benzo[f]quinoline structure **(7a-f)** subjected to antimicrobial testing.

Compus / R=	*** The diameter of the inhibition zone (mm)**		
	S. aureus ATCC 25923	***E. coli ATCC 25922***	***C. albicans ATCC 10231***
4a / -NH_2	0	0	10.5±0.5
4b / -OMe	19.5±1.5	17±1.73	**20±1.5**
4c / -OEt	**20±1**	18.5±1.5	**22±1.25**
5a / -C_6H_5	18±1.5	13±1.5	**20±1.8**
5b / -$C_6H_4(CH_3)_p$	**20.5±1.5**	17±2	**21.5±1.8**
5c / -$C_6H_4(OCH_3)_p$	**21.5±1.73**	18±1.73	**22±1**
5d / -$C_6H_4(C_6H_5)_p$	15±1.5	13±1.73	17±1
5e / -$C_6H_4(CN)_p$	15±2.5	12.5±1.25	15±1.73
5f / -$C_6H_4(NO_2)_p$	15±2	14±2.6	17±1
5g / -$C_6H_4(Br)_p$	16±1.5	12±1.5	19±1.5
5h / -$C_6H_4(Cl)_p$	**21±1.5**	18±1.32	**22.5±1**

5i / -$C_6H_4(F)_p$	14±1.5	10.5±1.5	14±0.5
7a / -NH_2	0	0	0
7b / -OMe	0	0	0
7c / -OEt	0	0	0
7d / -$C_6H_4(C_6H_5)_p$	0	0	0
7e / -$C_6H_4(Cl)_p$	0	0	0
7f / -$C_6H_4(F)_p$	0	0	0
C+	44±1	46±1.33	21±1

All values represented in the table represent the average of the results of five experiments performed separately. Bold and underlined means **very active**, while underlined means **active**.
* Diameter of inhibition zone (mm); X + - SD, average of five measurements + - standard deviation. C +: Penicillin 10 IU for *Staphylococcus aureus*, carbenicillin 100 μg/mL for *Escherichia coli*, and nystatin 500,000 IU for *Candida albicans*.

The best antibacterial activity against the Gram-positive bacterium *Staphylococcus aureus* **ATCC 25923** is shown by quaternary benzo[*f*]quinolinium salts with an aliphatic residue **(4c),** aromatic substituted with *p*-methyl **(5b),** *p*-methoxy **(5c),** respectively *p*-chloro **(5h)** respectively**,** the diameter of the inhibition zone being around 21 mm. The same salts show good activity against the Gram-negative bacterium *Escherichia coli* **ATCC 25922**, the diameter of the zone of inhibition being around 17 mm. The quaternary salts with an aliphatic residue **(4b,c),** respectively with an aromatic residue **(5a,b,c,h)** show a very good antifungal activity against the fungus *Candida albicans* **ATCC 10231**, the diameter of the inhibition zone being around 22 mm.

In the next step of the antimicrobial testing, the MIC-minimum inhibitory concentration (MIC) was determined for the most active quaternary benzo*[f]*quinolinium salts with both aliphatic and aromatic residues, **4b,c** and **5a,b,c,d,e,h** respectively, using the standardised microdilution test procedure[75-78].The resulting MIC value is defined as the lowest concentration of antimicrobial salts under investigation that prevents visible growth of the test microorganism. The results obtained are listed in **table II.6**.

Table II.6 The minimum inhibitory concentration (MIC) for quaternary benzo[f]quinolinium salts with aliphatic residue **(4b, c)** and aromatic residue **(5a,b,c,d,e,h)** (μg/mL).

Stem	**MIC** (μg/mL)								
	C+	**4b**	**4c**	**5a**	**5b**	**5c**	**5d**	**5e**	**5h**
S. aureus ATCC 25923	0.5	1.56	0.39	0.195	0.195	**0.00304**	0.39	1.19	0.0975
E. coli ATCC 25922	0.25	1.56	0.78	0.195	0.195	**0.00152**	0.78	1.39	0.195
C. albicans ATCC 10231	1.56	3.12	0.78	0.139	0.195	**0.0575**	0.78	0.81	0.195

C +: Penicillin for *Staphylococcus aureus*, Carbenicillin for *Escherichia coli* and Nystatin for *Candida albicans*. Bold and underlined means **very active**, while underlined means **active**.

The inhibition zone diameter shown in **Table II.5**, MIC data in **Table II.6** and **Figures II.39, II.40, II.41** reveal some interesting observations and correlations between the structures of the tested compounds and their antimicrobial activity. The tested quaternary salts **(4a-c)** and **(5a-i),** respectively, have an excellent *quasi-non-selective* antifungal activity against the fungus *C. albicans*, a very good antibacterial activity against the Gram-positiv bacterium *S. aureus* and they are less active against the Gram-negative *E. coli*. The antifungal activity is significantly more pronounced in the aliphatic series **(4a-c)** compared to the aromatic one of the compounds **(5a-i),** which demonstrates a certain influence on the activity of the aliphatic substituent of the carbonyl group. In the aromatic series **(5a-i),** compounds **5h** [R = -$C_6H_4(Cl)_p$] and **5c** [R = -$C_6H_4(OCH_3)_p$] have the highest antifungal activity, which also indicates an influence of the substituent (chloro or methoxy) on the para position of the phenyl ring.

The same SAR (structure activity relationship) considerations are highlighted by the results obtained in antibacterial testing against *S. aureus* and *E. coli bacteria*. Finally, when comparing the two series of compounds tested, the quaternary benzo*[f]*quinolinium salts (**4a-c)** respectively **(5a-i)** and the cycloadducts with pyrolo-benzo*[f]*quinoline structure **(7a-f),** it can be seen that only the quaternary salts have antimicrobial activity while the cycloadducts tested are inactive, which means that to have antimicrobial activity it is better to have a mobile substituent bound to the nitrogen atom (case of quaternary salts) instead of a newly condensed ring (case of cycloadducts).

II.3.2. Anticancer properties of quaternary benzo[*f*]quinolinium salts and of some cycloadducts with pyrrolo-benzo[*f*]quinolinium structure

Some compounds with a benzo[*f*]quinoline skeleton have been tested for their anticancer properties. Thus, the anticancer activity of quaternary benzo[*f*]quinolinium salts with aliphatic residues **(4a-c)** and aromatic residues **(5b,c,d,h),** as well as some cycloadducts with pyrrolo-benzo[*f*]quinolinic structure **(7a- e), (17a-c), (19a-c)** was evaluated by the National Cancer Institute (NCI), USA, through their screening programme for anticancer agents **(figure II.42)** [69]. The anticancer testing *in vitro* used NCI 60 cell line screening includes 60 different human tumour cell lines representing different cancers such as leukaemia, melanoma and cancers of the lung, colon, brain, ovary, breast, prostate and kidney[91].

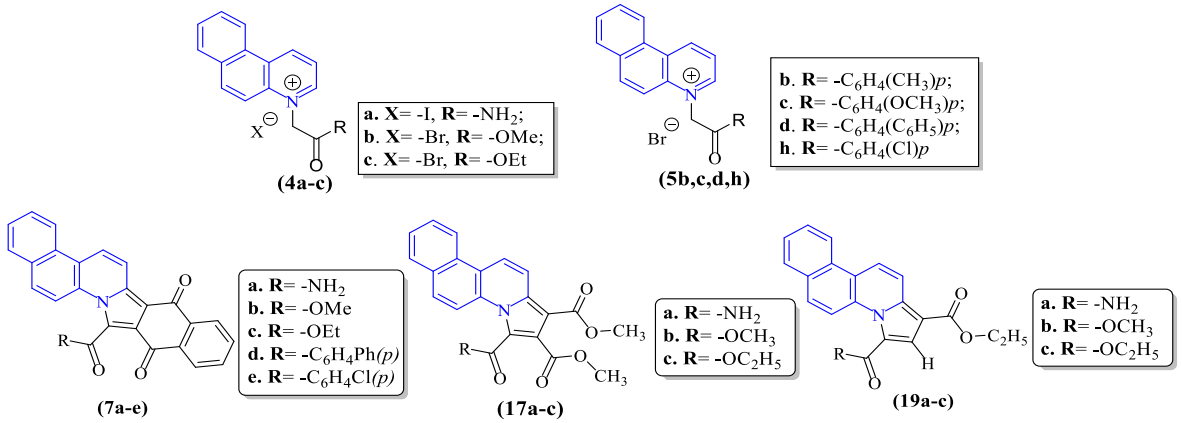

Figure II.42. The structure of quaternary benzo[*f*]quinolinium salts with aliphatic residues **(4a-c)** and aromatic residues **(5 b,c,d,h)** and of some cycloadducts with pyrrolo-benzo[*f*]quinolinic structure **(7a-e), (17a- c), (19a-c)** subjected to anticancer testing.

The raw results for compounds **5d** (benzo[*f*]quinolinium salt with *p*-phenyl substituted aromatic residue) as well as the cycloadduct with pyrrolo-benzo[f]quinolinic structure **17a** are highlighted in the appendices: **Annex 4** and **Annex 5** respectively.

The results of the anticancer tests at a single concentration of quaternary benzo[f]quinolinium salts with aliphatic residue **(4a-c)** and aromatic residue **(5 b,c,d,h)** are presented in **table II.7**.

Table II.7 The percentage of growth inhibition (PGI %, μM) [a] of quaternary benzo[*f*]quinolinium salts with aliphatic residue **(4a-c)** and aromatic **(5 b,c,d,h)** respectively in the anticancer test at a single concentration, compared to 60 NCI human cancer cell lines.

Section A

Cell type	**Quaternary salts / Percentage of growth inhibition (PGI%)[a]**						
	4a	**4b**	**4c**	**5b**	**5c**	**5d**	**5h**
Leukemia							
CCRF–CEM	0	3	4	72	48	68	41
HL–60 (TB)	0	20	0	**99**	78	**100**(62)[b]	70
K–562	0	34	5	**92**	**84**	**100**(26)[b]	**83**
MOLT–4	0	33	0	**86**	68	**100**(3)[b]	67
RPMI–8226	0	40	9	**95**	75	**93**	67
SR	4	40	15	**98**	66	**100**(28)[b]	**88**
Non-small cell lung cancer							
A549/ATCC	0	9	3	76	62	59	43
EKVX	11	10	12	71	57	59	43
HOP–62	0	0	4	64	56	56	28
HOP–92	0	15	0	**100**(8)[b]	**88**	**93**	**87**
NCI–H226	9	22	19	64	41	-	32
NCI–H23	2	29	3	73	72	56	41

NCI–H322M	0	5	0	57	31	36	37
NCI–460	0	0	0	**96**	**81**	73	46
NCI–H522	0	11	4	78	71	64	25
Colon cancer							
COLO 205	0	7	0	**94**	74	75	53
HCC–2998	1	0	0	**83**	52	**88**	54
HCT–116	0	48	1	**88**	70	**85**	**81**
HCT–15	0	0	0	43	13	47	23
HT29	0	0	0	**88**	**80**	**87**	79
KM12	0	15	5	74	65	72	23
SW–620	0	3	0	**81**	64	72	51
Central nervous system cancer							
SF–268	0	26	18	57	62	52	16
SF–295	0	5	0	77	70	66	53
SF–539	1	23	9	75	47	39	65
SNB–19	0	32	24	74	68	74	44
SNB–75	3	13	2	57	18	29	2
U251	3	40	28	**82**	72	70	46
Cell type	**Quaternary salts / Percentage of growth inhibition (PGI%)[a]**						
	4a	**4b**	**4c**	**5b**	**5c**	**5d**	**5h**
Leukemia							
CCRF–CEM	0	3	4	72	48	68	41
HL–60 (TB)	0	20	0	**99**	78	**100**(62)[b]	70
K–562	0	34	5	**92**	**84**	**100**(26)[b]	**83**
MOLT–4	0	33	0	**86**	68	**100**(3)[b]	67
RPMI–8226	0	40	9	**95**	75	**93**	67
SR	4	40	15	**98**	66	**100**(28)[b]	**88**
Non-small cell lung cancer							
A549/ATCC	0	9	3	76	62	59	43
EKVX	11	10	12	71	57	59	43
HOP–62	0	0	4	64	56	56	28
HOP–92	0	15	0	**100**(8)[b]	**88**	**93**	**87**
NCI–H226	9	22	19	64	41	-	32
NCI–H23	2	29	3	73	72	56	41
NCI–H322M	0	5	0	57	31	36	37
NCI–460	0	0	0	**96**	**81**	73	46
NCI–H522	0	11	4	78	71	64	25
Colon cancer							
COLO 205	0	7	0	**94**	74	75	53
HCC–2998	1	0	0	**83**	52	**88**	54
HCT–116	0	48	1	**88**	70	**85**	**81**
HCT–15	0	0	0	43	13	47	23
HT29	0	0	0	**88**	**80**	**87**	79
KM12	0	15	5	74	65	72	23
SW–620	0	3	0	**81**	64	72	51

Section B

Central nervous system Cell type	**Quaternary salts / Percentage of growth inhibition (PGI%)[a]**						
Melanoma							
LOX IMVI	5	9	4	**100**(24)[b]	54	**89**	**82**
MALME–3M	6	32	4	**87**	66	57	35
M14	0	21	1	**83**	62	76	39
MDA–MB–435	0	33	0	**87**	63	61	38
SK–MEL–2	0	0	0	64	44	37	13
SK–MEL–28	0	6	0	56	33	26	21
SK–MEL–5	0	63	21	**100**(89)[b]	**100**(32)[b]	**100**(35)[b]	62
UACC–257	0	8	0	**95**	**85**	47	48
UACC–62	1	43	8	68	44	34	36
Ovarian cancer							
IGROV1	0	14	0	69	33	52	51
OVCAR–3	0	36	0	70	48	69	37
OVCAR–4	0	39	4	**80**	67	**91**	37
OVCAR–5	0	0	3	69	42	42	47
OVCAR–8	0	1	0	78	74	74	49
NCI/ADR–RES	0	0	0	19	2	14	13
SK–OV–3	0	12	2	66	50	47	27
Kidney cancer							
786–0	0	13	2	66	33	46	48
A498	0	0	0	25	0	0	0
ACHN	0	0	0	50	21	44	33
CAKI–1	10	12	4	47	21	67	27
RXF 393	1	0	0	**94**	44	68	46
SN12C	0	15	6	**85**	**83**	74	46
TK–10	0	0	0	59	27	31	35
UO–31	21	16	16	70	44	71	68
Prostate cancer							
PC–3	9	29	2	**81**	73	86	64
DU–145	0	0	0	64	44	58	32
Breast cancer							
MCF7	4	39	13	**88**	**82**	**90**	61
MDA–MB–231/ATCC	0	21	0	76	60	58	48
HS 578T	0	12	1	73	41	56	32
BT–549	0	0	0	79	67	44	32
T–47D	0	10	3	56	62	64	35
MDA–MB–468	17	**85**	**76**	**100**(10)[b]	**97**	**100**(10)[b]	69

[a] percent of growth inhibition (PGI) at a single dose of 10 μM against 60 cell lines; [b]Cytotoxic effect; the percentage of lethality is represented in parentheses; the most active compounds are highlighted in **bold** and **red**

The results of anticancer tests at a single concentration of cycloadducts with pyrrolo-benzo[*f*]quinoline structure **(7a-e), (17a-c), (19a-c)** are presented in **table II.8**.

Table II.8 Growth inhibition percentage (PGI %, μM) [a] of cycloadducts with pyrrolo-benzo[*f*]quinoline structure **(7a-e)**, **(17a-c)**, **(19a-c)** in the anticancer test, at a single concentration, compared to 60 NCI human cancer cell lines.

Section A

Cell type	**Cycloadducts / Percentage of growth inhibition (PGI%)[a]**										
	17a	**19a**	**17b**	**19b**	**17c**	**19c**	**7a**	**7b**	**7c**	**7d**	**7e**
Leukemia											
CCRF–CEM	26	0	0	0	0	0	0	2	0	0	0
HL–60 (TB)	0	0	0	0	3	0	0	1	0	0	0
K–562	17	0	0	0	0	0	0	0	0	0	0
MOLT–4	10	0	0	3	0	0	0	0	0	0	0
RPMI–8226	33	0	0	13	0	2	0	0	0	0	0
SR	28	24	5	20	20	5	4	9	6	0	0
Non-small cell lung cancer											
A549/ATCC	0	0	3	0	0	0	0	0	0	7	0
EKVX	8	0	3	20	0	0	3	3	0	0	3
HOP–62	0	0	0	20	0	7	0	8	0	1	8
HOP–92	25	0	3	17	0	0	0	0	0	0	1
NCI–H226	32	0	0	22	13	20	0	8	0	-	0
NCI–H23	26	0	0	17	0	0	5	7	3	2	4
NCI–H322M	25	0	0	0	0	0	0	1	2	0	0
NCI–460	43	0	0	0	0	0	0	0	0	0	0
NCI–H522	6	0	0	1	1	0	0	4	0	0	7
Colon cancer											
COLO 205	19	0	0	1	0	0	0	0	0	0	0
HCC–2998	0	0	0	0	0	0	0	0	0	4	0
HCT–116	19	0	2	11	0	8	0	0	0	0	0
HCT–15	23	0	2	0	0	0	0	0	0	0	0
HT29	5	0	0	1	0	0	0	0	0	0	0
KM12	8	0	0	1	0	0	0	1	0	0	0
SW–620	11	0	0	8	0	0	0	1	0	0	0
Central nervous system cancer											
SF–268	11	0	0	0	0	0	0	0	0	0	0
SF–295	15	0	7	16	1	8	0	3	0	0	1
SF–539	30	0	1	3	0	8	2	9	0	0	12
SNB–19	17	0	19	11	0	5	1	10	0	0	4
SNB–75	29	0	4	20	0	3	0	4	0	0	13
U251	2	0	3	8	1	0	1	0	0	1	0

Section B

Melanoma											
LOX IMVI	25	0	0	9	0	6	5	5	2	0	10
MALME–3M	26	0	4	5	6	0	3	12	0	0	0
M14	12	0	0	0	0	0	0	6	0	4	0
MDA–MB–435	7	0	1	1	0	0	0	0	0	0	0
SK–MEL–2	0	0	0	0	0	0	0	0	0	0	0
SK–MEL–28	10	0	0	0	0	0	0	0	0	0	0
SK–MEL–5	29	0	2	0	0	0	0	0	0	0	0
UACC–257	0	0	0	0	0	0	0	1	0	10	0
UACC–62	7	0	6	20	17	10	0	8	0	2	3
Ovarian cancer											
IGROV1	24	0	0	19	0	1	0	0	14	0	0
OVCAR–3	5	0	24	0	0	9	0	0	0	0	0
OVCAR–4	36	0	0	34	2	20	0	0	0	0	0
OVCAR–5	5	0	0	1	0	0	0	0	0	0	0
OVCAR–8	26	0	0	4	0	0	0	0	0	0	0
NCI/ADR–RES	21	1	0	8	0	4	1	2	0	0	0
SK–OV–3	0	0	0	10	0	12	0	7	0	0	5
Kidney cancer											
786–0	11	0	0	4	4	8	0	0	0	0	0
A498	0	0	0	0	0	0	0	0	0	0	0
ACHN	28	0	0	**41**	0	17	0	0	8	0	18
CAKI–1	9	0	0	38	0	15	5	9	11	4	8
RXF 393	22	5	25	0	0	1	0	8	0	1	-
SN12C	17	0	4	22	0	0	1	0	0	4	0
TK–10	0	0	0	0	3	0	0	0	0	0	0
UO–31	37	8	12	**45**	21	33	18	26	26	10	30
Prostate cancer											
PC–3	23	0	1	19	5	3	9	0	11	0	5
DU–145	26	0	0	0	0	0	0	0	0	0	0
Breast cancer											
MCF7	36	7	15	10	8	10	23	14	10	0	7
MDA–MB–231/ATCC	**42**	0	0	11	0	1	6	4	5	0	10
HS 578T	9	0	7	19	0	6	0	2	0	1	7
BT–549	30	0	0	0	0	0	0	0	0	0	0
T–47D	21	0	6	3	19	1	0	10	0	7	0
MDA–MB–468	29	0	10	0	7	0	2	2	0	5	0

[a] percent growth inhibition (PGI) at a single dose of 10 μM against 60 cell lines.

Based on the results presented in **Tables II.7** and **II.8**, it is observed that the most active compounds are the benzo[*f*]quinolinium salts **5b** and **5d**, respectively, which are quaternary

salts containing an aromatic chain. The compound **5b** (substituted *p*-CH3) shows almost *non-selective* activity against all types of cancer cells (except for one type of ovarian cancer cells and one type of renal cancer cells), displaying excellent growth inhibition of 50-100% and significant lethality against four different types of cancer cells (non-small cell lung cancer HOP-92, (8%), melanoma LOX IMVI (24%), SK-MEL-5 (89%) and breast cancer MDA-MB-468 (10%)).

The quaternary salt **5d** (substituted *p*-C_6H_5) demonstrates *highly selective* activity against *leukemia*, showing 100% growth inhibition and cytotoxicity against four different cell types: HL-60 (TB) (letalitate 62%); K-562 (letalitate 26%); MOLT-4 (letalitate 3%); SR (28% letalitate). Another noteworthy activity is that of the quaternary salt **5c** (substituted *p*-OCH_3), which exhibits a percent growth inhibition of 80-100% against nine different cell types including leukemia K-562 (PGI = 84%), non-small cell lung cancer HOP-92 (PGI = 88%), non-small cell lung cancer NCI-460 (PGI = 81%), colon cancer HT29 (PGI = 80%), melanoma SK-MEL-5 (PGI = 100%, L = 32%), melanoma UACC- 257 (PGI = 85%), renal cancer SN12C (PGI = 83%), breast cancer MCF7 (PGI = 82%) and breast cancer MDA-MB-468 (PGI = 97%).

Quaternary salt **4b** (with *methyl ester* residue) is the most active of the aliphatic series, showing good anticancer activity against *breast cancer* cell type MDA-MB-468 (PGI = 85%). Among the pyrrolo-benzo[*f*]quinoline cycloadducts tested, the most promising results are obtained by cycloadduct **17a** (with *amido* residue), showing a PGI of about 10–40% against all cancer cells.

The results in **Tables II.7** and **II.8** highlight the fact that the quaternary salts show better anticancer activity compared to the tested cycloadducts. Considering the structure-activity relationship (SAR), certain observations can be made regarding the tested compounds:

- ✓ some compounds show high activity against several cancer cell lines, while others have a more selective effect;
- ✓ quaternary salts with aromatic residue **5 b,c,d,h** have better activity compared to salts with aliphatic residue **4a-c**;
- ✓ the major factor influencing the anticancer activity is the existence of the substituent in the *para* position of the benzoyl fragment. Thus, compounds containing a *methyl* or *phenyl* group show the greatest activity. Moreover, the presence of a *methoxy* or *chlorine* moiety seems to have a favorable effect on the activity;

- ✓ the activity of the quaternary salts is superior to that of the cycloadducts tested, an aspect that could be attributed to the presence of a positively charged nitrogen atom in the molecule;
- ✓ cycloadducts with a pyrrolo-benzo[*f*]quinoline structure **(17a-c, 19a-c)** show better activity compared to derivatives with an isoindolo-benzo[*f*]quinoline structure **(7a-e).** This aspect suggests that a single fused cycle is preferable to two for a superior anticancer activity.

The benzo[*f*]quinolinium salt from aromatic series with *p*-phenyl moiety **5d** was selected for NCI 5-dose screening (stage two), which may provide valuable insight into its potential efficacy as an anticancer agent[96].

The results obtained in the second phase of the anticancer tests for benzo[f]quinolinium quaternary salt 5d are given in Table II.9 and Annex 5..

Table II.9. 50% cell growth inhibition (GI_{50}, μM)of **5d** quaternary salt in anticancer assay at five different concentrations (step 2) against 60 NCI human cancer cell lines.

Cell type	**Quaternary salt/ 50% cell growth inhibition (GI_{50})**	***Cell type***	**Quaternary salt/ 50% cell growth inhibition (GI_{50})**
	5d		**5d**
Leukemia		***Ovarian cancer***	
CCRF–CEM	3.28	IGROV1	8.36
HL–60 (TB)	**1.72**	OVCAR–3	4.85
K–562	**2.25**	OVCAR–4	**2.99**
MOLT–4	3.37	OVCAR–5	8.17
RPMI–8226	**2.66**	OVCAR–8	4.06
SR	**2.73**	NCI/ADR–RES	**1.66**
Non-small cell lung cancer		SK–OV–3	6.32
A549/ATCC	4.49	***Kidney cancer***	
EKVX	4.68	786–0	9.73
HOP–62	4.70	A498	**1.47**
HOP–92	-	ACHN	**1.03**
NCI–H226	**2.43**	CAKI–1	3.34
NCI–H23	4.61	RXF 393	**2.72**
NCI–H322M	**1.22**	SN12C	3.13
NCI–460	4.62	TK–10	**1.27**
NCI–H522	4.14	UO–31	6.47
Colon cancer		***Prostate cancer***	
COLO 205	3.61	PC–3	**2.50**
HCC–2998	3.28	DU–145	7.23
HCT–116	3.85	***Breast cancer***	
HCT–15	4.46	MCF7	**2.96**

HT29	3.26	MDA–MB–231/ATCC	4.55
KM12	4.15	HS 578T	**1.06**
SW–620	4.42	BT–549	5.03
Central nervous system cancer		T–47D	3.56
SF–268	9.97	MDA–MB–468	**2.04**
SF–295	3.58		
SF–539	9.56	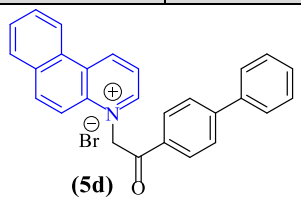 **(5d)** Quaternary salt structure tested in stage 2	

[a] molar concentration of the test compound inhibiting 50% of tumour cell growth (GI_{50}) at five different doses 100, 10, 1.0, 0.1 respectively 0.01 μM against 60 cell lines.

From the results presented in the above table it is evident that the quaternary salt of the tested aromatic series **5d** (substituted p-C6H5), shows GI_{50} values between 1.02-2.99 μM for 18 different cell lines. Thus, the best anticancer activity of inhibiting cell growth by 50% is shown against renal cancer with GI_{50} values for four different cell lines: A498 of 1.47 μM, ACHN of 1.03 μM, RXF 393 of 2.72 μM respectively TK-10 of 1.27 μM. Also this quaternary salt has a 50% satisfactory cell growth inhibition activity against leukaemia for four cell lines (GI_{50} = 1.72 μM for HL-60 (TB), GI_{50} = 2.25 μM for K-562, GI_{50}= 2.66 μM for RPMI-8226 respectively GI_{50} = 2.73 μM for SR). The best inhibition activity is against skin cancer (melanoma) for the SK-MEL-2 cell line showing GI_{50} = 1.02 μM.

CONCLUSIONS

➢ The results of the research carried out in the framework of the PhD thesis "**AZAHETEROCYCLES WITH CONDENSATED NUCLEES. SYNTHESIS, STRUCTURE, PROPERTIES**" can be concluded as follows:

➢ Eleven quaternary benzo[*f*]quinolinium salts were synthesized, 4 with aliphatic residue **(4a-d)**, and 9 with aromatic skeleton **(5a-i),** the salts with aliphatic residue **(4a-c)** respectively the quaternary salt with aromatic residue **(5c)** have been previously reported in the literature, in this thesis an efficiency of the chemical synthesis was achieved (increased yield, reduced amount of solvent, reduced working time).

➢ By reacting quaternary salts with aliphatic residue **(4a-c)** and aromatic residue **(5d,h,i),** respectively, with a symmetrically substituted cyclic alkene dipolarophile, namely 1,4-naphthoquinone, in chloroform using triethylamine as base, 6 cycloadducts with pyrolo-benzo[*f*]quinoline structure **(7a-f)** were obtained, with yields in the product of interest ranging from 42%-62%.

➢ Treating the quaternary benzo[*f*]quinolinium salt with p-nitro **(5f)** residue with NEMI respectively NFMI in 1,2-butyleneoxide, used both as solvent and acceptor of hydrobromic acid, 2 cycloadducts with tetrahydropyrrolo-benzo[*f*]quinolinic structure **(13a-b)** were obtained.

➢ Starting from quaternary benzo[*f*]quinolinium salts with aliphatic residue **(4a-d)**, by [3+2] dipolar cycloaddition reactions with symmetrically substituted activated alkynes (DMAD), a series of 4 new cycloadducts with pyrolo-benzo[*f*]quinolinic structure **(17a-d)** was obtained, using 1,2-butyleneoxide both as solvent and as HBr acceptor. Cycloadducts with pyrolo-benzo[*f*]quinolinic structure **(17b,c)** have been previously reported in the literature, in this thesis we succeeded in improving the working conditions, using 1,2-butyleneoxide both as solvent and as HBr acceptor, previously the reactions took place in chloroform using triethylamine as base, as well as increasing the yield in the product of interest. Previously cycloadducts **(17b,c)** were characterized only by infrared spectroscopy, in the current research the spectral characterization of all cycloadducts with pyrolo-benzo[*f*]quinoline structure **(17a-d)** was performed using nuclear magnetic resonance spectroscopy, infrared spectroscopy, high resolution mass spectrometry, as well as single crystal X-ray (for compound **17b**).

➢ The research also included [3+2] dipolar cycloaddition reactions of benzo[*f*]quinolinium salts with aliphatic residue **(4a-c)** with ethyl propiolate (non-symmetrically substituted activated alkyne) in 1,2-butyleneoxide, yielding 3 cycloadducts with pyrolo-benzo[*f*]quinolinic

structure **(19a-c)** with yields in the product of interest (50%-68%). Cycloadducts with pyrolo-benzo[*f*]quinolinic structure **(19a-c)** have been previously reported in the literature, in this thesis it was possible to improve the working conditions, using 1,2-butyleneoxide both as solvent and as HBr scavenger, previously the reactions took place in chloroform using triethylamine as base, in this way reducing the working time and increasing the yield in the desired compound. Also previously cycloadducts **(19b,c)** were characterized only by infrared spectroscopy, in the current research spectral characterization of all cycloadducts **(19a-c)** was performed using nuclear magnetic resonance spectroscopy, infrared spectroscopy, high resolution mass spectrometry.

- Compounds with benzo[*f*]quinolinic skeleton were subsequently subjected to antimicrobial and antifungal testing. The antimicrobial activity of quaternary benzo[*f*]quinolinic salts with aliphatic **(4a-c)** as well as aromatic **(5a, i)** residues was found to be clearly superior to the pyrolo-benzo[*f*]quinolinic cycloadducts **(7a-f)** tested. The best antibacterial activity against Staphylococcus aureus ATCC 25923 was shown by salt **(4c)** with aliphatic residue and **(5b, c, h)** with aromatic residue, the diameter of the zone of inhibition being around 21 mm. The same salts also show good activity against Gram-negative Escherichia coli ATCC 25922. The salts with aliphatic residue **(4b,c)** and with aromatic residue **(5a,b,c,h)** show very good antifungal activity against the fungus C. albicans ATCC 10231, the diameter of the zone of inhibition being around 22 mm.
- The anticancer activity of quaternary benzo[*f*]quinolinium salts with aliphatic residue **(4a-d),** respectively with aromatic skeleton **(5 b,c,d,h),** as well as some cycloadducts with pyrolo-benzobenzo[*f*]quinolinic structure **(7a-e), (17a-c), (19a-c)** has been evaluated by (NCI), USA, through their screening program for anticancer agents.
- The most active were found to be the benzo[*f*]quinolinium **(5b,d)** salts containing an aromatic chain. Compound **5b** (substituted *p*-CH3) shows almost non-selective activity against all types of cancer cells (except one type of ovarian cancer cells and one type of renal cancer cells), showing excellent growth inhibition of 50-100% and significant lethality against four different cancer cell types (non-small cell lung cancer HOP-92, (8%), melanoma LOX IMVI (24%), SK-MEL-5 (89%) and breast cancer MDA-MB-468 (10%)).
- Benzo[*f*]quinolinium **5d** salt (substituted *p*-C6H5) shows highly selective activity against leukaemia with 100% growth inhibition and cytotoxicity against four different cell types: HL-60 (TB) (62% lethality); K-562 (26% lethality); MOLT-4 (3% lethality); SR (28% lethality).

➢ Another noteworthy activity is quaternary salt **5c** (substituted *p*-OCH3), which shows 80-100% percent growth inhibition against nine different cell types, including leukemia K-562 (PGI = 84%), non-small cell lung cancer HOP-92 (PGI = 88%), non-small cell lung cancer NCI-460 (PGI = 81%), colon cancer HT29 (PGI = 80%), melanoma SK-MEL-5 (PGI = 100%, L = 32%), melanoma UACC- 257 (PGI = 85%), kidney cancer SN12C (PGI = 83%), breast cancer MCF7 (PGI = 82%) and breast cancer MDA-MB-468 (PGI = 97%).

➢ Quaternary salt **4b** (with methyl ester residue) is the most active of the aliphatic series, showing good anticancer activity against the breast cancer cell type MDA-MB-468 (PGI = 85%). Of the cycloadducts with pyrolo-benzo[*f*]quinoline structure tested, the most promising results are obtained by cycloadduct **17a** (with amido residue), showing a PGI of about 10-40% against all cancer cells.

- Benzo[*f*]quinolinium **5d** salt (substituted *p*-C_6H_5) has been selected for NCI screening with 5 doses (stage 2), which may provide valuable information on its potential efficacy as an anticancer agent. The quaternary salt of the tested aromatic series **5d** (substituted *p*-C_6H_5), shows GI_{50} values ranging from 1.02-2.99 μM for 18 different cell lines. The best inhibitory activity was against skin cancer (melanoma) for the SK-MEL-2 cell line.
- The results of the thesis "AZAHETEROCYCLES WITH CONDENSATED NUCLEES. SYNTHESIS, STRUCTURE, PROPERTIES" have been published in two scientific articles, in Web of Science journals with impact factor as well as in five papers disseminated in the form of presentations (oral/poster) at conferences in the country and abroad. (The list of personal contributions is attached at the end of the thesis).

BIBLIOGRAPHY

1. Katrintsky, A.R.; Taylor, R. Chapter 11. Compounds Containing Two or More Six-Membered Rings. In *Advances in Heterocyclic Chemistry*; Academic Press, Inc., San Diego, California, **1990**; Volum 47, pp 353–398.
2. Ram, V.J.; Sethi, A.; Nath, M.; Pratap, R. Chapter 2. Six-Membered Heterocycles. In *The Chemistry of Heterocycles: Chemistry of Six to Eight Membered N, O, S, P and Se*; Dennis, S., McCloskey, E.M. Eds.; Elsevier, Amsterdam, Netherlands, **2019**; pp 101–106. https://doi.org/10.1016/B978-0-12-819210-8.00002-3.
3. Amăriucăi-Mantu, D.; Mangalagiu, I.I.; Antoci, V. Synthesis of Benzo[*f*]Quinoline and its Derivatives: Mini Review, *Med & Analy Chem Int J* **2019**, 3(1), 1-10. DOI: 10.23880/macij-16000133.
4. Goel, A.; Kumar, V.; Singh, S.P.; Sharma, A.; Prakash, S.; Singh, C.; Anand, R.S., Non-aggregating solvatochromic bipolar benzo[*f*]quinolines and benzo[*a*]acridines for organic electronics, *J Mater Chem* **2012**, 22, 14880-14888.
5. Bahuguna, R.P.; Joshi B.C.; Mangal, H.N., Studies on benzoquinoline derivatives: preparation and antimicrobial activityof azo-derivatives of arylthiobenzo[*f*]quinoline, J *Indian Chem Soc* **1992**, 69(7), 401–402.
6. Monge, A.; Alvarez, E.; San Martín, C.; Nadal, E.; Ruiz, I.; Font, M.; Martínez-Irujo, J.J.; Santiago, E.; Prieto, I.; Lasarte, J.J.; Sarobe, P.; Borrás, F., Synthesis and evaluation of new Reissert analogs as HIV-1 RT inhibitors. 2. Benzo[*f*]quinoline and pyridine derivatives, *Drug Des Discov* **1997**, 14(4), 291-303.
7. Yang, S.; Hua, W.; Wu, Y.; Hu, T.; Wang, F.; Zhang, X.; Zhang, F., Site-selective Synthesis of Functionalized Dibenzo[*f,h*]quinolines and their derivatives involving cyclic diaryliodonium salts via Decarboxylative Annulation Strategy, Chem Comm **2018**, 54(26), 3239-3242.
8. Clem, W.J.; Hamilton, C.S., Nitro and Aminobenzo[*f*]quinolines and Derivatives, *J Am Chem Soc* **1940**, 62, 2349-2352.
9. Loader, C,E.; Timmons, C.J., Studies in Pthochemistry. Part II. The Photocyclisation of Stilbazoles to Azaphenanthrenes, *J Chem Soc* **1966**, (C), 1078-1081.
10. Kulmer, P.L.; Dybas, R.A., Photochemical Cyclizations. I. Preparation of Benzo[*f*]quinolines by Photolisis of 2-Stilbazole Derivatives, *JOC* **1970**, 35(1), 125-131.
11. Ramann, G.A.; Cowen, B.J. Quinoline synthesis by improved Skraup–Doebner–Von Miller reactions utilizing acrolein diethyl acetal, *Tetrahedron Lett* **2015**, 56, 6436–6439.

12. Manske, R.H.; Kulka, M., The Skraup Synthesis of Quinolines, *Organic Reactions* **2004**, 7, 59-98.
13. Wang, X.S.; Zhou, J.; Yang, K.; Yao, C.S., Yb (OTf) 3: an efficient catalyst for the synthesis of 3-arylbenzo[*f*]quinoline-1,2-dicarboxylate derivatives via imino-Diels–Alder reaction, *Tetrahedron Letters* **2010**, 51(43), 5721-5723.
14. Shiri, M.; Zolfigol, M.A.; Kruger, H.G.; Tanbakouchian, Z., Friedländer annulation in the synthesis of azaheterocyclic compounds. *In Advances in Heterocyclic Chemistry*, Academic Press, **2011**, Vol. 102, pp. 139-227.
15. Hamada, Y.; et al., *Chem Pharm Bull Jpn* **1979**, 27, 1535.
16. Wang, X.S.; Li, Q.; Yao, C.S.; Tu, S.J., *Eur J Chem* **2008**, 3513.
17. Asnani, A.J.; Sahare, S., *Asian J Pharm Clin Res* **2013**, 6, 303.
18. Miarzaro, G.; Via, L.D.; Garcia-Argaez, A.N.; Via, M.D.; Chilin, A., *Biorog Med Chem Lett* **2016**, 26, 4875.
19. Bejan, V.; Mangalagiu, I.I., *Rev Chim (Bucharest)* **2011**, 62, 199.
20. Khusnutdinov, R.I.; Bayguzina, A.R.; Mukminov, R.R.; Dzhemilev, U.M., *ARKIVOC* **2016**, 63.
21. Hamada, Y.; Takeuchi, I., *J Org Chem* **1977**, 42, 4209.
22. Hamada, Y.; Sugiura, M., *Yakugaku Zasshi* **1978**, 98, 1081.
23. Clem, W.J.; Hamilton, C.F., *J Am Chem Soc* **1940**, 62, 2349.
24. Saeki, K.I.; Tomomitsu, M.; Kawazoe, Y.; Momota, K.; Kimoto, H., *Chem Pharm Bull* **1996**, 44, 2254.
25. Mamane, V.; Louerat, F.; Fort, Y., *Lett Org Chem* **2010**, 7, 90.
26. Barltrop, J.A.; Taylor, D.A.H., *J Chem Soc* **1951**, 108.
27. Vierhapper, F.W.; Eliel, E.L., *J Org Chem* **1975**, 40, 2729.
28. Cardellni, M.; Cingolani, G.M.; Claudi, F.; Cristalli, G.; Gulini, U.; Martelli, S., *J Org Chem* **1982**, 47, 688.
29. Krishnan, S.; Kuhn, D.G.; Hamilton, G.A., *J Am Chem Soc* **1977**, 91, 8121.
30. Tyagi, R.P.; Joshi, B.C., *Bull Chem Soc Jpn* **1972**, 45, 2507
31. Der, H.; Kumbhani, J.; Patel, M.; Ram, K.; Joshi, D.; Chatrabhuji, P., Synthesis, characterization and biological evaluation of novel 3-amino-1-(phenyl)benzo[*f*]quinoline-3-carbonitrile derivatives, *International Journal of Chemical Studies* **2016**, 4(5), 05-09.
32. Elenich, O.V.; Lytvyn, R.Z.; Blinder, O.V.; Skripskaya, O.V.; Lyavinets, O.S.; Pitkovych, Kh.E.; Obushak, M.D.; Yagodinets, P.I., Synthesis and antimicrobial activity of 3-phenyl-

1-methylquinolin-2-one derivatives, *Pharmaceutical Chemistry Journal* **2019**, 52(12), 969-974.

33. Dikusar, E.A.; Kadutskii, A.P.; Kozlov, N.G.; Yuvchenko, A.P.; Melȼnichuk L.A., Salts of *spiro*-derivatives of benzo[*f*]quinoline and several natural carboxylic acids, *Chemistry of Natural Compounds* **2006**, 42(1), 118-120.
34. Tietze, L.F.; Herzig, T.; Fecher, A., Novel prodrugs von 6-hydroxy-2,3-dihydro-1H-indoles, 5-hydroxy-1,2-dihydro-3H-pyrrolo[3,2-E] indoles and 5-hydroxy-1,2-dihydro-3H-benzo(*e*)indoles as well as of 6-hydroxy-1,2,3,4-tetrahydro-benzo[*f*]quinoline derivatives for use in selective cancer therapy, Patent US 2004/0033962 A1, **2004**.
35. Park, G.Y.; Wilson, J.J.; Song, Y.; Lippard, S.J., Phenanthriplatin, a monofunctional DNA-binding platinum anticancer drug candidate with unusual potency and cellular activity profile, *PNAS* **2012**, 109(30), 11987-11992.
36. Kim, H.S.; Joo, C.W.; Pyo, B.; Lee, J.; Suh, M.S., Improvement of viewing angle dependence of the white organic light emitting diodes with tandem structure by introduction of nanoporous polymer films, *Organic Electronics* **2017**, 40, 88-96.
37. Noguchi, Y.; Miyazaki, Y.; Tanaka, Y.; Sato, N.; Nakayama, Y.; Schmidt, T.D.; Brütting, W.; Ishii, H., Charge accumulation at organic semiconductor interfaces due to a permanent dipole moment and its orientational order in bilayer devices, *Journal of Applied Physics* **2012**, 111, 114508.
38. Park, S.R.; Seo, J.S.; Ahn,Y.; Lee, J.H.; Suh, M.C., Thermally stable benzo[*f*]quinoline based bipolar host materials for green phosphorescent OLEDs, *Organic Electronics* **2018**, 63, 194-199.
39. Seo, J.; Park, S.R.; Kim, M.; Suh, M.C.; Lee, J., The role of electron-transporting Benzo[*f*]quinoline unit as an electron acceptor of new bipolar hosts for green PHOLEDs, *Dyes and Pigments* **2019**, 162, 959-966.
40. Goel, A.; Kumar, V.; Singh, S.P.; Sharma, A.; Prakash, S.; Singh, C.; Anand, R.S., Non-aggregating solvatochromic bipolar benzo[*f*]quinolines and benzo[*a*]acridines for organic electronics, *J Mater Chem* **2012**, 22, 14880.
41. Witting, G.; Fellestschin, G., *Ann* **1944**, 55,133,.
42. Jonson, W. A., *Ylid Chemistry*, Academic Press, N.Y., **1966**.
43. Zugrăvescu, I.; Petrovanu, M., *N-Ylid Chemistry*, McGraw-Hill, London, **1976**.
44. Zugrăvescu, I.; Petrovanu, M., *Chimia N-ilidelor*, Ed. Acad., **1974**.
45. Ingold, C. K.; Jessop, J. A., *Chem Soc* **1929**, 2357.
46. Krollpfeiffer, F.; Muller, A., *Ber* **1933**, 66, 739.

47. Kröhnke, F., *Chem Ber* **1935,** 68, 1177.

48. Zugrăvescu, I., *Rev Chim Bucuresti* **1970**, 21, 669.

49. Huisgen, R.; Grashey, R.; Gotthardt, H.; Schmidt, R., 1,3-Dipolar additions of sydnones to alkynes. A new route into the pyrazole series. *Angew Chem Int Ed Engl* **1962**, 1(1), 48-49

50. Padwa, A. (Ed.), in: *1,3-Dipolar Cycloaddition Chemistry*, Vol. 1, Chapter 1 (ed. by A. Padwa, pp. 1 – 176); Vol. 2, Chapter 12 (ed. by A. Padwa, pp. 277-406) and Chapter 13 (ed. by K.N. Houk, K. Yamaguchi, pp. 407-450) and the references cited therein, John Wiley & Sons, New York, **1984**, ISBN 047108364X, 9780471083641.

51. Houben-Weyl, *Organische Stickstoff-Verbindungen mit einer C,N-Doppelbindungen*, Thieme Stuttgart, New York, **1991**, E14b, pp. 100- 1200.

52. Epiotis, N.D. Theory of Organic Reactions, Springer, Berlin, **1978**, ISBN 978-3-642-66827-2.

53. Breugst, M.; Reissig, H.U., The Huisgen reaction: milestones of the 1,3-dipolar cycloaddition. *Angew Chem Int Ed* **2020**, 59(30), 12293–12307. doi.org/10.1002/anie.202003115

54. Amariucai-Mantu, D.; Mangalagiu, V.; Mangalagiu, I.I., [3 + n] Cycloaddition Reactions: A Milestone Approach for Elaborating Pyridazine of Potential Interest in Medicinal Chemistry and Optoelectronics. *Molecules* **2021**, 26, 3359. https://doi.org/10.3390/molecules26113359

55. Firestone, R.A., On the mechanism of 1,3-dipolar cycloadditions. *J Org Chem* **1968**, 33(6), 2285–2290.

56. Firestone, R.A., The low energy of concert in many symmetry-allowed cycloadditions supports a stepwise-diradical mechanism. *Int J Chem Kinet* **2013**, 45 (7), 415–428. doi: https://doi.org/10.1002/kin.20776

57. Tsuge, O.; Kanemasa, S.; Takenaka, S., Stereochemical study on 1,3-dipolar cycloaddition reactions of heteroaromatic *N*-ylides with symmetrically substituted cis and trans olefins. *Bull Chem Soc Jpn* **1985**, 58(11), 3137-3157. https://doi.org/10.1246/bcsj.58.3137

58. Caprosu, M.; Mangalagiu, I.I.; Sirbu-Maftei, D.; Olariu, I.; Petrovanu, M., Studies on pyridazinium ylides. II. Stereochemistry of 3+2 dipolar cycloadditions of E-Z olefins. *An Stiint Univ Al.I. Cuza Iasi* 1997, 5(s1c), 95-102. [*Chem Abstr* **2000**, 132, # 207816].

59. Mangalagiu, I.I.; Druta, I.; Constantinescu, M.; Humelnicu, I.; Petrovanu, M., Pyridazinium ylides. Regiochemistry. *Tetrahedron* **1996**, 52(26), 8853-8862. doi: 10.1016/0040-4020(96)00432-2

60. Caprosu, M.; Olariu, I.; Mangalagiu, I.I.; Constantinescu, M.; Petrovanu M., The regiochemistry of the cycloaddition of 4-R-phenacylpyridazinium ylides to nonsymmetrical substituted olefins. *Eur J Org Chem* **1999**, 12, 3501-3504.

61. Mangalagiu, I.I.; Mangalagiu, G.; Drochioiu, G.; Deleanu, C.; Petrovanu, M., 4-Methyl pyrimidinium ylides. Part 7: 3+2 dipolar cycloadditions to non-symmetrical substituted alkenes and alkynes. *Tetrahedron* **2003**, 59(1), 111-114. doi: 10.1016/S0040-4020(02)01453-9

62. Do Nhat Van; Rucinschi, E.; Druţă, I.; Zugrăvescu, I., *Bull Instit Politehnic Iaş*i, **1977**.

63. Bejan, V., *Azaheterocycles analogs of natural steroids obtained by conventional and unconventional methods*, Doctoral Thesis, "Al. I. Cuza" University of Iași, Faculty of Chemistry, Iași, **2010**.

64. Cristl, R.; Huisgen, R., *Chem Ber* **1975**, 106, 3345.

65. Huisgen, R.; Cristl, R., *Chem Ber* **1973**, 106, 3291.

66. Georgescu, E.; Draghici, C.; Iuhas, P.C.; Georgescu, F., A new approach for the synthesis of benzo[*f*]pyrrolo[1,2-a]-quinolines, *Arkivoc* **2005**, X, 95-104.

67. Moldoveanu, C.; Mangalagiu, I.; Zbancioc, G., Fluorescent Azasteroids through Ultrasound Assisted Cycloaddition Reactions. *Molecules* **2021**, *26*, 5098. https://doi.org/10.3390/molecules26165098

68. Antoci, V.; **Oniciuc, L.**; Amariucăi-Mantu, D.; Moldoveanu, C.; Mangalagiu, V.; Amarandei, A.M.; Lungu, C.N.; Dunca, S.; Mangalagiu, I.I.; Zbancioc, Ghe., Benzoquinoline Derivatives: A Straightforward and Efficient Route to Antibacterial and Antifungal Agents, *Pharmaceuticals* **2021**, 14, 335. https://doi.org/ 10.3390/ph14040335

69. **Oniciuc, L.**; Amariucai-Mantu, D.; Diaconu, D.; Mangalagiu, V.; Danac, R.; Antoci, V.; Mangalagiu, I.I., Benzoquinoline Derivatives: An Attractive Approach to Newly Small Molecules with Anticancer Activity, *Int J Mol Sci (International Journal of Molecular Sciences)* **2023**, 24, 8124. https://doi.org/10.3390/ijms24098124.

70. WHO Global Strategy for Containment of Antimicrobial Resistance. Available from:/WHO/ https://www.who.int/drugresistance/WHO_Global_Strategy_English.pdf

71. Silverman, R.B.; Holladay, M.W., *The organic chemistry of drug design and drug action*, 3rd Edition; Academic Press, London, 2014; ISBN: 9780123820303.

72. Brunton, L.; Knollmann, B.; Hilal-Dandan, R., *Goodman & Gilman's the pharmacological basis of therapeutics*, 13th Edition; McGraw-Hill, NY, USA, 2013; ISBN13: 9781259584732.

73. Eicher, T.; Hauptmann, S.; Speicher, A., *The Chemistry of Heterocycles: Structures, Reactions, Synthesis, and Applications*, 3rd Edition; Wiley-VCH: Weinheim, 2013; ISBN: 978-3-527-32747-8.

74. Methods for dilution antimicrobial susceptibility tests for bacteria that grow aerobically; approved standard, 11th Edition, CLSI document M07-A11, 2018. Clinical and Laboratory Standards Institute, Wayne, PA. Available from:
https://clsi.org/media/1928/m07ed11_sample.pdf

75. Kavanagh, A.; Ramu, S.; Gong, Y.; Copper, M.A.; Blaskovich, M.A.T. Effects of microplate type and broth additives on microdilution MIC susceptibility assays. *Antimicrob Agents Ch* **2019**, 63(1), 1-17.

76. Balouiri, M.; Sadiki M.; Ibnsouda K.S. Methods for in vitro evaluating antimicrobial activity. *J Pharm Anal* **2016**, *6*, 71-79

77. Thakur, D.; Sahani, K. In vitro antimicrobial activity and MIC of the extracellular ethyl acetate crude extract of endophytic fungi Fusarium sp. isolated from Tephrosia purpurea root. *Int J Pharm Pharm Sci* **2019**, 11(3), 48-53

78. Osaka, I.; Hefty, P.S. Simple resazurin-based microplate assay for measuring chlamydia infections. *Antimicrob Agents Ch* **2013**, 57(6), 2838-2840.

79. Vitaku, E.; Smith, D.T.; Njardarson, J.T., Analysis of the structural diversity, substitution patterns, and frequency of nitrogen heterocycles among US FDA approved pharmaceuticals. *J Med Chem* 2014, 57, 10257–10274, https://doi.org/10.1021/jm501100b.

80. WHO. Cancer. https://www.who.int/news-room/fact-sheets/detail/cancer.

81. NIH. Cancer Treatment. https://www.cancer.gov/about-cancer/treatment/types.

82. Abraham, J.; Staffurth, J., Hormonal therapy for cancer. *Medicine* 2016, 44(1), 30–33, https://doi.org/10.1016/j.mpmed.2015.10.014.

83. Esfahani, K.; Roudaia, L.; Buhlaiga, N.; Del Rincon, S.V.; Papneja, N.; Miller, W.H. Jr., A review of cancer immunotherapy: from the past, to the present, to the future. *Curr Oncol* 2020, 27 (Suppl 2), 87–97, doi: 10.3747/co.27.5223.

84. Czogała, W.; Czogała, M.; Kwiecinska, K.; Bik-Multanowski, M.; Tomasik, P.; Hałubiec, P.; Łazarczyk, A.; Miklusiak, K.; Skoczen, S., The Expression of Genes Related to Lipid Metabolism and Metabolic Disorders in Children before and after Hematopoietic Stem Cell Transplantation—A Prospective Observational Study. *Cancers* 2021, 13, 3614, https://doi.org/10.3390/ cancers13143614.

85. Kinch, M.S. An analysis of FDA–approved drugs for oncology. *Drug Discov Today* 2014, 19, 1831–1835, https://doi.org/10.1016/j.drudis.2014.08.007.

86. Magalhaes, L.G.; Ferreira, L.L.G.; Andricopulo, A.D., Recent Advances and Perspectives in Cancer Drug Design, *An Acad Bras Cienc* 2018, 90, 1233-1236, https://doi.org/10.1590/0001-3765201820170823.

87. Barreca, M.; Spanò, V.; Raimondi, M. V.; Tarantelli, C.; Spriano, F.; Bertoni, F.; Barraja, P.; Montalbano, A. Recurrence of the oxazole motif in tubulin colchicine site inhibitors with anti-tumor activity. *Eur J Med Chem Rep* 2021, 1, 100004, https://doi.org/10.1016/j.ejmcr.2021.100004.

88. El-Sherief, H.A.M.; Youssif, B.G.M.; Bukhari, S.N.A.; Abdel-Aziz, M.; Abdel-Rahman, H.M. Novel 1,2,4-triazole derivatives as potential anticancer agents: Design, synthesis, molecular docking and mechanistic studies. *Bioorganic Chemistry* 2018, 76, 314–325, https://doi.org/10.1016/j.bioorg.2017.12.013

89. Barreca, M.; Spanò, V.; Rocca, R.; Bivacqua, R.; Abel, A.C.; Maruca, A.; Montalbano, A.; Raimondi, M.V.; Tarantelli, C.; Gaudio, E.; Cascione, L.; Rinaldi, A.; Bai, R.; Steinmetz, M.O.; Prota, A.E.; Alcaro, S.; Hamel, E.; Bertoni, F.; Barraja, P., Development of [1,2] oxazoloisoindoles tubulin polymerization inhibitors: Further chemical modifications and potential therapeutic effects against lymphomas. *Eur J Med Chem* 2022, 243, 114744. doi: 10.1016/j.ejmech.2022.114744.

90. Vieira, A.M.G.; Silvestre, O.F.; Silva, B.F.B.; Ferreira, C.J.O.; Lopes, I.; Gomes, A.C.; Espiña, B.; Sárria, M.P., pH-sensitive nanoliposomes for passive and CXCR-4-mediated marine yessotoxin delivery for cancer therapy. *Nanomedicine* 2022, 17(10), 717-739, https://doi.org/10.2217/nnm-2022-0010.

91. Cell Lines in the In Vitro Screen. Available online: https://dtp.cancer.gov/discovery_development/nci-60/cell_list.htm

92. Shoemaker, H.R. The NCI60 human tumour cell line anticancer drug screen. *Nat Rev Cancer* **2006**, 6, 813–823, https://doi.org/10.1038/nrc1951.

93. Skehan. P.et al. New colorimetric cytotoxicity assay for anticancer–drug screening. *J Natl Cancer Inst* **1990**, 82, 1107–1112., https://doi.org/10.1093/jnci/82.13.1107.

94. Boyd, R.B. The NCI In Vitro Anticancer Drug Discovery Screen. In: Teicher B.A. (eds) Anticancer Drug Development Guide. Cancer Drug Discovery and Development. Humana Press: Totowa, NJ, USA, **1997**; pp. 23–42, https://doi.org/10.1007/978-1-4615-8152-9_2.

95. The COMPARE program. Available online: http://dtp.nci.nih.gov/docs/compare/compare.html

96. The Standard NCI/DTP Methodology of The In Vitro Cancer Screen. Available online: https://dtp.cancer.gov/discovery_development/nci-60/methodology.htm

97. Dolomanov, O.V.; Bourhis, L.J.; Gildea, R.J.; Howard, J.A.K.; Puschmann, H. OLEX2: A complete structure solution, refinement and analysis program. *J App. Crystallogr* **2009**, 42, 339–341, https://doi.org/10.1107/S0021889808042726

98. Sheldrick, G.M. SHELXT–Integrated space–group and crystal–structure determination. *ActaCrystallogr Sect A Found Crystallogr* **2015**, 71, 3–8, https://doi.org/10.1107/S2053273314026370

99. Sheldrick, G.M. Crystal structure refinement with SHELXL. *ActaCrystallogr Sect C Struct Chem* **2015**, 71, 3–8, https://doi.org/10.1107/S2053229614024218

LIST OF PERSONAL CONTRIBUTIONS IN THE THESIS

- ***Scientific articles published in extenso in Web of Science cited journals with impact factor***

1. **Oniciuc, L.**; Amariucai-Mantu, D.; Diaconu, D.; Mangalagiu, V.; Danac, R.; Antoci, V.; Mangalagiu, I.I., Benzoquinoline Derivatives: An Attractive Approach to Newly Small Molecules with Anticancer Activity, *Int J Mol Sci (International Journal of Molecular Sciences)* **2023**, 24, 8124.

https://doi.org/10.3390/ijms24098124. **(I.F.= 5.6)**

2. Antoci, V.; **Oniciuc, L.**; Amariucăi-Mantu, D.; Moldoveanu, C.; Mangalagiu, V.; Amarandei, A.M.; Lungu, C.N.; Dunca, S.; Mangalagiu, I.I.; Zbancioc, Ghe., Benzoquinoline Derivatives: A Straightforward and Efficient Route to Antibacterial and Antifungal Agents, *Pharmaceuticals* **2021**, 14, 335. https://doi.org/ 10.3390/ph14040335 **(I.F.= 4.6)**

- ***As well as disseminated in the form of presentations (oral/poster) at conferences at home and abroud***

1. Mangalagiu, I.I.; **Oniciuc, L.**; Antoci, V.; Mangalagiu, V.: Benzo[*f*]quinoline Derivatives: a NMR Study Concerning Structure Determination, *Adriatic NMR*, Croatia, June 1-4, **2023**. (Poster presentation, P09, pag. 55).
1-Adriatic_NMR_2023_Book_of_Abstracts.pdf
https://adriatic-nmr-conference.hkd.hr/

2. Antoci, V.; Amăriucăi-Mantu, D.; Diaconu, D.; **Oniciuc, L.;** Dănac, R.; Ciobanu, C.; Mangalagiu, V.; Mangalagiu, I.: Anticancer activity of new hybrid derivatives with benzo[f]quinoline skeleton, *CUKUROVA 9th INTERNATIONAL SCIENTIFIC RESEARCHES CONFERENCE*, October 9-11, Adana, Turcia, **2022**, pag 148, book of abstract, (oral presentation/on-line), www.iksadkongre.net

3. **Oniciuc, L.**; Antoci, V.; Amariucai-Mantu, D.; Diaconu, D.; Ciobanu, C.; Mangalagiu, V.; Mangalagiu, I.I.: Novel benzo[*f*]quinoline derivatives with antimicrobial properties, *Scientific communication session of students, masters and PhD students*, Edition XIII, pag. 22, 28 October **2022**, Iasi, România. (Oral Presentation CO-09)
https://www.chem.uaic.ro/ro/manifestari/scssmd2022.html

4. Antoci, V.; Zbancioc, Ghe.; **Oniciuc, L.**; Amăriucăi-Mantu, D.; Moldoveanu, C.; Dănac, R.; Ciobanu, C.; Mangalagiu, V.; Mangalagiu, I.I.:

BENZO[*F*]QUINOLINIUM SALTS: ANTIBACTERIAL AND ANTIFUNGAL ACTIVITIES, *New frontiers in natural product chemistry*, June 4-5, **2021**, Chișinău, Moldova. (Poster presentation, pag. 21).
http://dx.doi.org/10.19261/nfnpc.2021.ab14
https://www.chem.uaic.ro/ro/manifestari/scssmd2022.html

https://ichem.md/en/scientific-seminar-new-frontiers-natural-product-chemistry-2021
Book of Abstracts / editors: Aculina Arîcu, Veaceslav Kulcițki, Editura: Institute of Chemistry, ISBN 978-9975-3336-7-2 (PDF). DOI: 10.19261/nfnpc.2021.

5. Amariucai-Mantu, D.; **Oniciuc, L.**; Diaconu, D.; Ciobanu, C.; Mangalagiu, I.I.; Mangalagiu, V.; Antoci, V.: Novel tetrahyropyrrolo-benzo[*f*]quinoline compounds: synthesis and characterizations. *4th International Conference on Sustainable Science and Technology* (ICSuSaT-2021) 01-02 october **2021**, ONLINE-TURKEY, poster 34. (poster presentation). https://icsusat.net/icsusat-2021